SI Materials and Methods

Construction of mutant strains. Gene deletions (1, 2) and antibiotic cassette removals (3) were performed by P1 *vir* phage transduction using Keio mutants, as previously described 22. BN1 was generated by deletion of *pagP* from BN0, an *lpxT* and *eptA* double mutant (1, 4). Deletion of all three genes resulted in a strain producing >95% of the prototypical, hexa-acylated *bis*-phosphorylated lipid A species (SI Appendix Fig. S2). To double the potential lipid A profiles that one set of enzymes could yield, BN2 was generated by removal of the Kan^R cassette and deletion of *lpxM* from BN1. Strains were confirmed by PCR, ^{32}P radiolabeling, and MS (SI Appendix Table S2, Fig. S2) (5).

Plasmid construction and growth conditions. Six genes, *lpxE, lpxF, lpxO, lpxR, pagL,* and *pagP,* were cloned into pQLinkN (for primers see SI Appendix Table S2), as previously described (6). Transformation of BN1 and BN2 with the plasmids yielded the 61 strains in Fig. 2c. All strains were grown at 37°C in Luria-Bertani Broth supplemented with 100 μg/ml ampicillin where appropriate and 50 μM to 1 mM IPTG with an optimized isopropyl β-D-1-thiogalactopyranoside (IPTG) concentration between 50 μM and 1 mM, as determined by TLC analysis of enzyme activity.

Isolation of lipid A. ^{32}P radiolabeled lipid A was isolated from 7 ml cultures for analysis by TLC as previously described (5). Densitometry was calculated using Quantity One software. For MS, lipid A was prepared from 15 ml cultures (7) and analyzed using a MALDI-TOF/TOF (ABI 4700 Proteomics Analyzer) mass spectrometer in the negative ion linear mode as previously described (7). For strains expressing both phosphatases, LpxE and LxpF, lipids were detected in the positive mode.

TLR Signaling Assays. HEK-Blue™ hTLR4, HEK-Blue™ hTLR2, and THP1-XBlue™-MD2-CD14 cell lines were purchased from Invivogen and maintained according to their specifications. Whole cell aliquots and LPS samples were serial diluted for assays as previously described (7) with the following modification: whole cell stimulation assays were done in 30 µg/ml chloramphenicol instead of 50 U/ml – 50 µg/ml Pen-Strep to maintain a bacteriostatic effect. At least two biological replicates were each done in triplicate and one representative set was shown here, normalized to data for the BN1 pQLinkN strain.

Purification of individual lipid A species. Purification of 3-*O*-deacyl-4′-monophosphoryl lipid A produced by strain BN1/pELP was performed by reverse-phase chromatography as described previously (8) with ~ 0.4-0.6 mg of the target lipid obtained per liter of culture. The amount of purified lipid A was quantified by phosphate determination as previously described (9). Based upon TLC analysis, approximately 1/3rd of the lipid A synthesized is 3-*O*-deacyl-4′-monophosphoryl lipid A. Assuming there are 10^9 CFU/ml of bacteria at an OD_{600} of 1.0 and ~10^6 lipid A molecules per cell (4), the maximum yield of the target lipid would be ~1 mg/L of culture.

Isolation and quantification of LPS. LPS was isolated from 13 of the strains as previously described (7). Quantification was achieved using the 3-deoxy-D-*manno*-octulosonic acid (Kdo) colorimetric assay (10) to normalize the samples to 0.5 mg/ml using *E. coli* K12 LPS (LPS EK-Ultrapure, Invivogen) as a standard.

Whole cell bacterial sample preparation. Cells for assays were prepared by growing a diluted overnight culture to an OD_{600} of 1.0 and washing with sterile phosphate

buffered saline (PBS) to remove lysed cells or vesicle fragments. Cell pellets were gently resuspended in 5 mls of PBS, and the OD_{600} was measured. 5 x 10^9 cells were harvested by centrifugation, gently resuspended in 1 ml PBS and aliquoted for storage at -80° C. CFU plating after storage at -80° C confirmed equivalent cell counts between samples.

Lipopolysaccharide stimulation assays and cytokine quantification. THP-1 human monocytes (ATCC) were maintained according to ATCC's specifications. THP-1 monocytes were differentiated into macrophages and stimulated for 24 h with 100 ng/ml LPS as previously described (11). LPS samples were quantified as described above and normalized to the number of LPS molecules. Culture supernatants from triplicate wells were harvested and sent to Ocean Ridge Biosciences (Palm Beach Gardens, FL) for Luminex quantification of the cytokines: TNF-α, IL-1β, IL-6, IL-8, G-CSF, RANTES and MCP-1.

Mouse IgG and cytokine quantification. All procedures were performed according to IACUC and institutional guidelines. Monophosphoryl lipid A (MPLA) was purchased from Invivogen and is referred to as MPL, for simplicity. Female Balb/cJ mice (Jackson) (7 mice/group), 6-8 weeks old, were bled from the tail vein (~20 µl) prior to primary injection (day -1) and on day 28. Serum was stored at -20° C for further analysis. Emulsions were prepared as described previously (12), and on day 1 mice were immunized subcutaneously into the backpad with 50 µl of an emulsion of 30 ug lysozyme from chicken egg white (HEL) with 6 pM of purified lipid A, determined by phosphate quantification as previously described (9). Secondary and final immunizations were performed intraperitoneally on day 21 and day 35, respectively,

with 50 µl of the same emulsions. On day 36, serum was collected by heart puncture for Luminex cytokine analysis.

Serum IgG titers were determined by ELISA serial dilution. Serum dilutions from 1/200 through 1/437000 were captured on HEL coated high binding ELISA plates (Corning Costar 3590) and detected with 1/5000 anti-Mouse IgG HRP (Jackson Immuno, 115-065-209). Plates were analyzed with GraphPad Prism software and titers were determined as the point where the non-linear fitted curve determined 3-fold signal above background.

Statistical analysis. Statistical analysis was performed using one-tailed T-tests. P-values were calculated with an $n \geq 3$, $\alpha=0.05$ or 0.01, as reported in the supplementary figure legends for TLR4 assays and n=7, $\alpha=0.05$ for IgG titer analysis. Error bars on graphs refer to standard deviation.

References

1. Herrera CM, Hankins JV, & Trent MS (2010) Activation of PmrA inhibits LpxT-dependent phosphorylation of lipid A promoting resistance to antimicrobial peptides. *Molecular microbiology* 76(6):1444-1460.
2. Baba T*, et al.* (2006) Construction of Escherichia coli K-12 in-frame, single-gene knockout mutants: the Keio collection. *Molecular systems biology* 2:2006-2008.
3. Datsenko KA & Wanner BL (2000) One-step inactivation of chromosomal genes in Escherichia coli K-12 using PCR products. *Proceedings of the National Academy of Sciences of the United States of America* 97(12):6640-6645.
4. Raetz CR, Reynolds CM, Trent MS, & Bishop RE (2007) Lipid A modification systems in gram-negative bacteria. *Annual review of biochemistry* 76:295-329.
5. Tran AX*, et al.* (2006) The lipid A 1-phosphatase of Helicobacter pylori is required for resistance to the antimicrobial peptide polymyxin. *Journal of bacteriology* 188(12):4531-4541.
6. Scheich C, Kummel D, Soumailakakis D, Heinemann U, & Bussow K (2007) Vectors for co-expression of an unrestricted number of proteins. *Nucleic acids research* 35(6):e43.

7. Hankins JV*, et al.* (2011) Elucidation of a novel Vibrio cholerae lipid A secondary hydroxy-acyltransferase and its role in innate immune recognition. *Molecular microbiology*.
8. Raetz CR*, et al.* (2006) Kdo2-Lipid A of Escherichia coli, a defined endotoxin that activates macrophages via TLR-4. *Journal of lipid research* 47(5):1097-1111.
9. Gonzalez-Romo P, Sanchez-Nieto S, & Gavilanes-Ruiz M (1992) A modified colorimetric method for the determination of orthophosphate in the presence of high ATP concentrations. *Analytical biochemistry* 200(2):235-238.
10. Marolda CL, Lahiry P, Vines E, Saldias S, & Valvano MA (2006) Micromethods for the characterization of lipid A-core and O-antigen lipopolysaccharide. *Methods in molecular biology* 347:237-252.
11. Brett PJ*, et al.* (2007) Burkholderia mallei expresses a unique lipopolysaccharide mixture that is a potent activator of human Toll-like receptor 4 complexes. *Molecular microbiology* 63(2):379-390.
12. Ulrich JT, Cieplak W, Paczkowski NJ, Taylor SM, & Sanderson SD (2000) Induction of an antigen-specific CTL response by a conformationally biased agonist of human C5a anaphylatoxin as a molecular adjuvant. *Journal of immunology* 164(10):5492-5498.

Table S1. Bacterial strains and plasmids used in this study.

Strain or plasmid	Genotype or description	Source or reference
Strains		
W3110	Wild type, F^- I^- rph-1 INV(*rrnD, rrnE*)1 *rph-1*	*E. coli* Genetic Stock center (Yale)
MLK1067	W3110 *lpxM*::Ω*cam*	[1]
CMR300	W3110 (*kdtA*::*kan*) pWMsbA	[2]
BN0	W3110 Δ*eptA,* Δ*lpxT*	This work
BN1	BN0 Δ*pagP*	This work
BN2	BN1 Δ*lpxM::kan*	This work
Plasmids		
pQLinkN	Vector containing a tac promotor, Amp^r	[3]
pE	pQLinkN containing *lpxE*	This work
pF	pQLinkN containing *lpxF*	This work
pL	pQLinkN containing *pagL*	This work
pO	pQLinkN containing *lpxO*	This work
pP	pQLinkN containing *pagP*	This work
pR	pQLinkN containing *lpxR*	This work
pEF	pQLinkN containing *lpxE, lpxF*	This work
pEL	pQLinkN containing *lpxE, pagL*	This work
pEO	pQLinkN containing *lpxE, lpxO*	This work
pEP	pQLinkN containing *lpxE, pagP*	This work
pER	pQLinkN containing *lpxE, lpxR*	This work
pFL	pQLinkN containing *lpxF, pagL*	This work
pFP	pQLinkN containing *lpxF, pagP*	This work
pFR	pQLinkN containing *lpxF. lpxR*	This work
pLO	pQLinkN containing *pagL, lpxO*	This work
pLP	pQLinkN containing *pagL, pagP*	This work
pLR	pQLinkN containing *pagL, lpxR*	This work
pOP	pQLinkN containing *lpxO, pagP*	This work
pOR	pQLinkN containing *lpxO, lpxR*	This work
pPR	pQLinkN containing *pagP, lpxR*	This work
pEFL	pQLinkN containing *lpxE, lpxF, pagL*	This work
pEFP	pQLinkN containing *lpxE, lpxF, pagP*	This work
pEFR	pQLinkN containing *lpxE, lpxF, lpxR*	This work
pELO	pQLinkN containing *lpxE, pagL, lpxO*	This work
pELP	pQLinkN containing *lpxE, pagL, pagP*	This work
pELR	pQLinkN containing *lpxE, pagL, lpxR*	This work
pEOP	pQLinkN containing *lpxE, lpxO, pagP*	This work
pEPR	pQLinkN containing *lpxE, pagP, lpxR*	This work
pFLP	pQLinkN containing *lpxR, pagL, pagP*	This work
pFLR	pQLinkN containing *lpxF, pagL, lpxR*	This work
pFPR	pQLinkN containing *lpxF, pagP, lpxR*	This work
pLOP	pQLinkN containing *pagL, lpxO, pagP*	This work
pLOR	pQLinkN containing *pagL, lpxO, lpxR*	This work
pLPR	pQLinkN containing *pagL, pagP, lpxR*	This work
pOPR	pQLinkN containing *lpxO, pagP, lpxR*	This work
pEFLP	pQLinkN containing *lpxE, lpxF, pagL, pagP*	This work
pEFLR	pQLinkN containing *lpxE. lpxF, pagL, lpxR*	This work
pEFPR	pQLinkN containing *lpxE, lpxF, pagP, lpxR*	This work
pELOP	pQLinkN containing *lpxE. pagL, lpxO, pagP*	This work
pELOR	pQLinkN containing *lpxE. pagL, lpxO, lpxR*	This work
pELPR	pQLinkN containing *lpxE, pagL, pagP, lpxR*	This work
pEOPR	pQLinkN containing *lpxE, lpxO, pagP, lpxR*	This work

pFLPR	pQLinkN containing *lpxF. pagL, pagP, lpxR*	This work
pLOPR	pQLinkN containing *pagL, lpxO, pagP, lpxR*	This work

Table S2. Primers used in this study.

Primer name	Primer sequence
LpxEBamHIfor	5′- GCGGATCCATGCTCAAACAGACATTA -3′
LpxEBamHIrev	5′- GCGCGGCCGCCTAAATAATCTCTCTATT -3′
LpxFBamHIfor	5′- GCGGATCCTTGGCAAGATTTCATATC -3′
LpxFBamHIrev	5′- GCGCGGCCGCTCAATATTCTTTTTTACG -3′
PagLBamHIfor	5′- GCGGATCCATGTATATGAAGAGAATA -3′
PagLBamHIrev	5′- GCGCGGCCGCTCAGAAATTATAACTAAT -3′
LpxOEcoRIfor	5′- GCGAATTCATGTTCGCAGCAATCATT -3′
LpxOBamHIrev	5′- GCGGATCCTCAGAGGAGGCTGAAAAG -3′
PagPBamHIfor	5′- GCGGATCCATGAACGTGAGTAAATAT -3′
PagPNotIrev	5′- GCGCGGCCGCTCAAAACTGAAAGCGCAT -3′
LpxRBamHIfor	5′- GCGGATCCATGAACAAATACAGCTAT -3′
LpxRNotIrev	5′- GCGCGGCCGCTCAGAAGAAGAAGGTGAT -3′

References

1. Karow, M. & Georgopoulos, C. Isolation and characterization of the Escherichia coli msbB gene, a multicopy suppressor of null mutations in the high-temperature requirement gene htrB. *Journal of bacteriology* **174**, 702-710 (1992).
2. Reynolds, C.M. & Raetz, C.R. Replacement of lipopolysaccharide with free lipid A molecules in Escherichia coli mutants lacking all core sugars. *Biochemistry* **48**, 9627-9640 (2009).
3. Scheich, C., Kummel, D., Soumailakakis, D., Heinemann, U. & Bussow, K. Vectors for co-expression of an unrestricted number of proteins. *Nucleic acids research* **35**, e43 (2007).

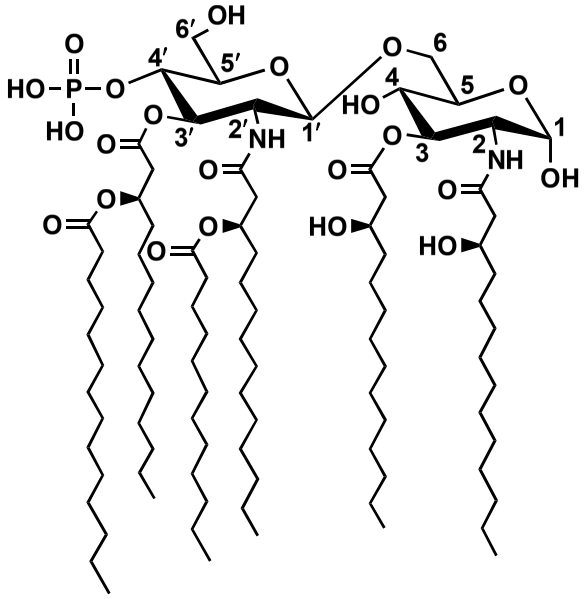

4′-monophosphoryl
lipid A (*E. coli*)

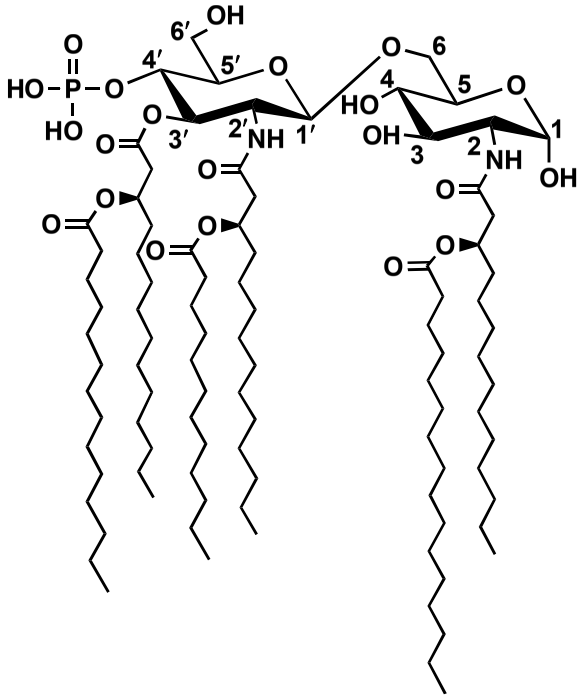

3-*O*-deacyl-4′-monophosphoryl
lipid A (MPL)

Fig. S1. Chemical structures of 4′-monophosphoryl lipid A and of 3-*O*-deacyl-4′-monophosphoryl lipid A (MPL).

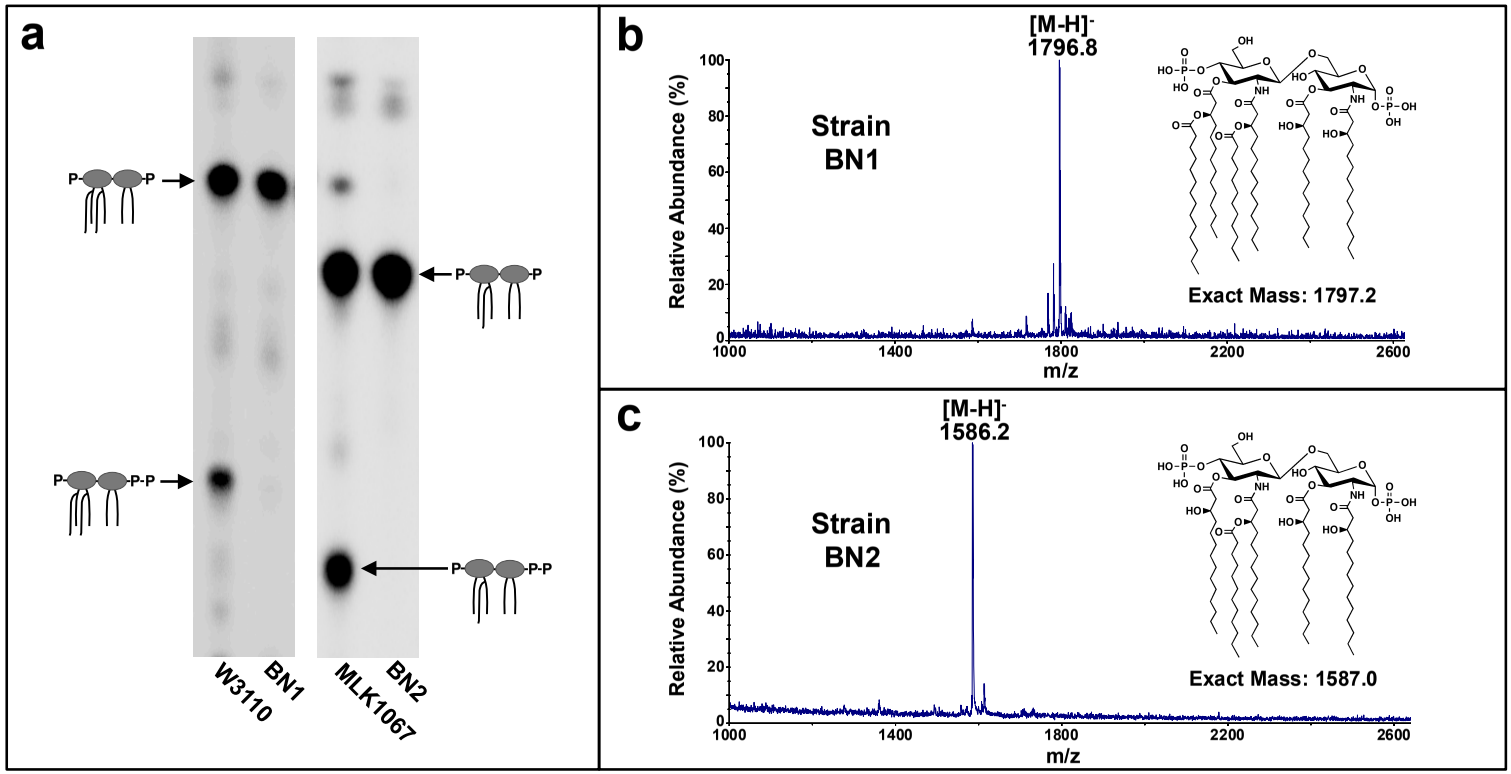

Fig. S2. Confirmation of mutant BN1 and BN2 strains. Radiolabeled lipid A of W3110 (*E. coli* K12), BN1, MLK1067, and BN2 was separated by TLC (a). W3110 synthesizes hexa-acylated lipid A with either two or three phosphate groups. BN1 is an *eptA, lpxT, pagP* mutant that loses the capacity to synthesize the lipid A species with three phosphate groups. These genes were deleted to eliminate modifications to the lipid A that occur under normal growth conditions. MLK1067 is an *lpxM* mutant of W3110 that synthesizes penta-acylated lipid A. BN2 is an *lpxM* mutant of the BN1 strain that produces only penta-acylated, *bis*-phosphorylated lipid A. b,c) BN1 and BN2 lipid A was analyzed by MALDI-TOF MS in negative ion linear mode. Ion peaks correspond to an appropriate exact mass (±1) for BN1 hexa-acylated lipid A with two phosphates at *m/z* 1797.2 and BN2 penta-acylated lipid A with two phosphates at *m/z* 1587.0.

Fig. S3, a

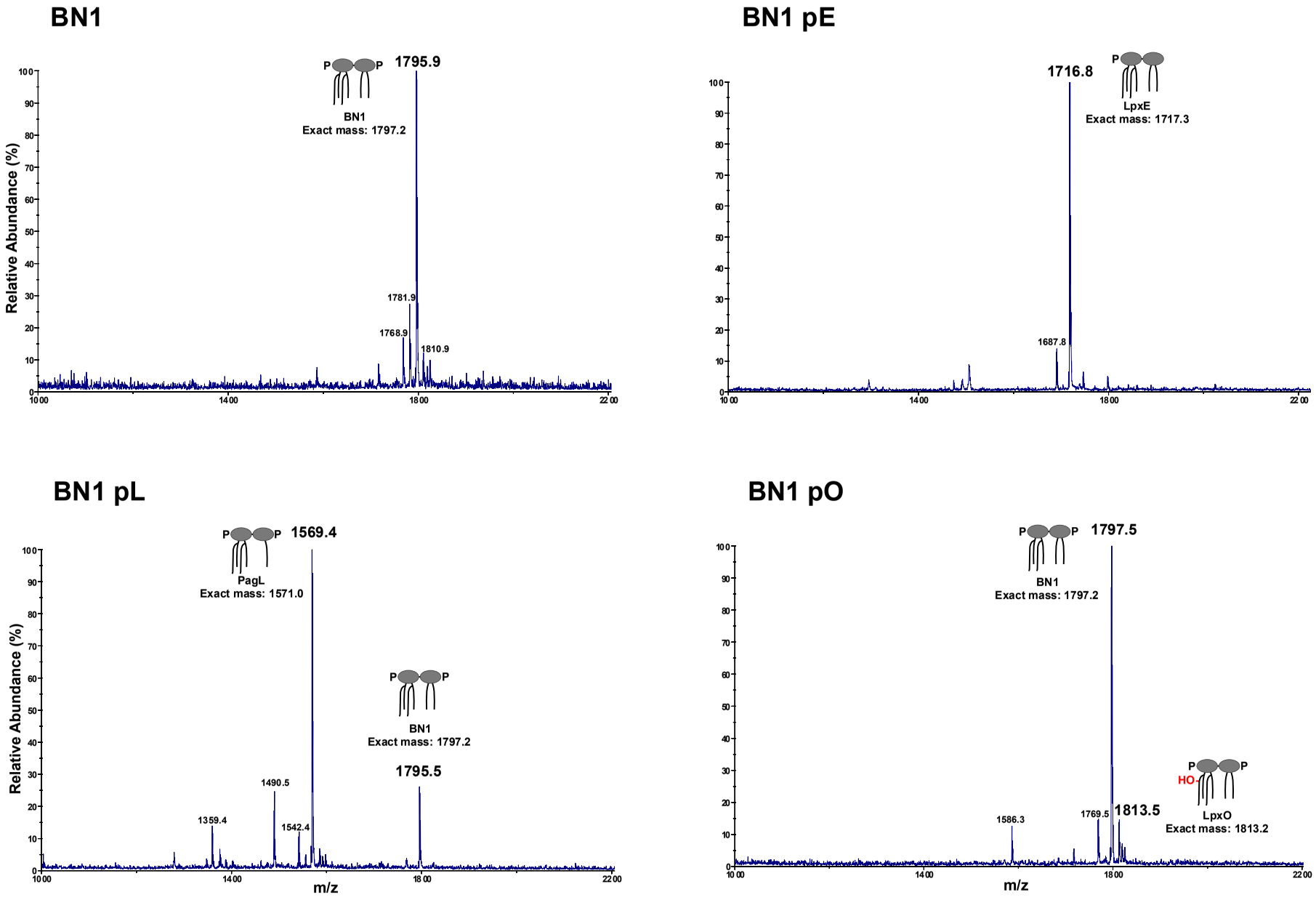
BN1
1795.9
BN1
Exact mass: 1797.2
1781.9
1768.9
1810.9
Relative Abundance (%)
BN1 pE
1716.8
LpxE
Exact mass: 1717.3
1687.8
BN1 pL
1569.4
PagL
Exact mass: 1571.0
BN1
Exact mass: 1797.2
1795.5
1490.5
1359.4
1542.4
m/z
BN1 pO
1797.5
BN1
Exact mass: 1797.2
HO
1586.3
1769.5
1813.5
LpxO
Exact mass: 1813.2

a, cont'd

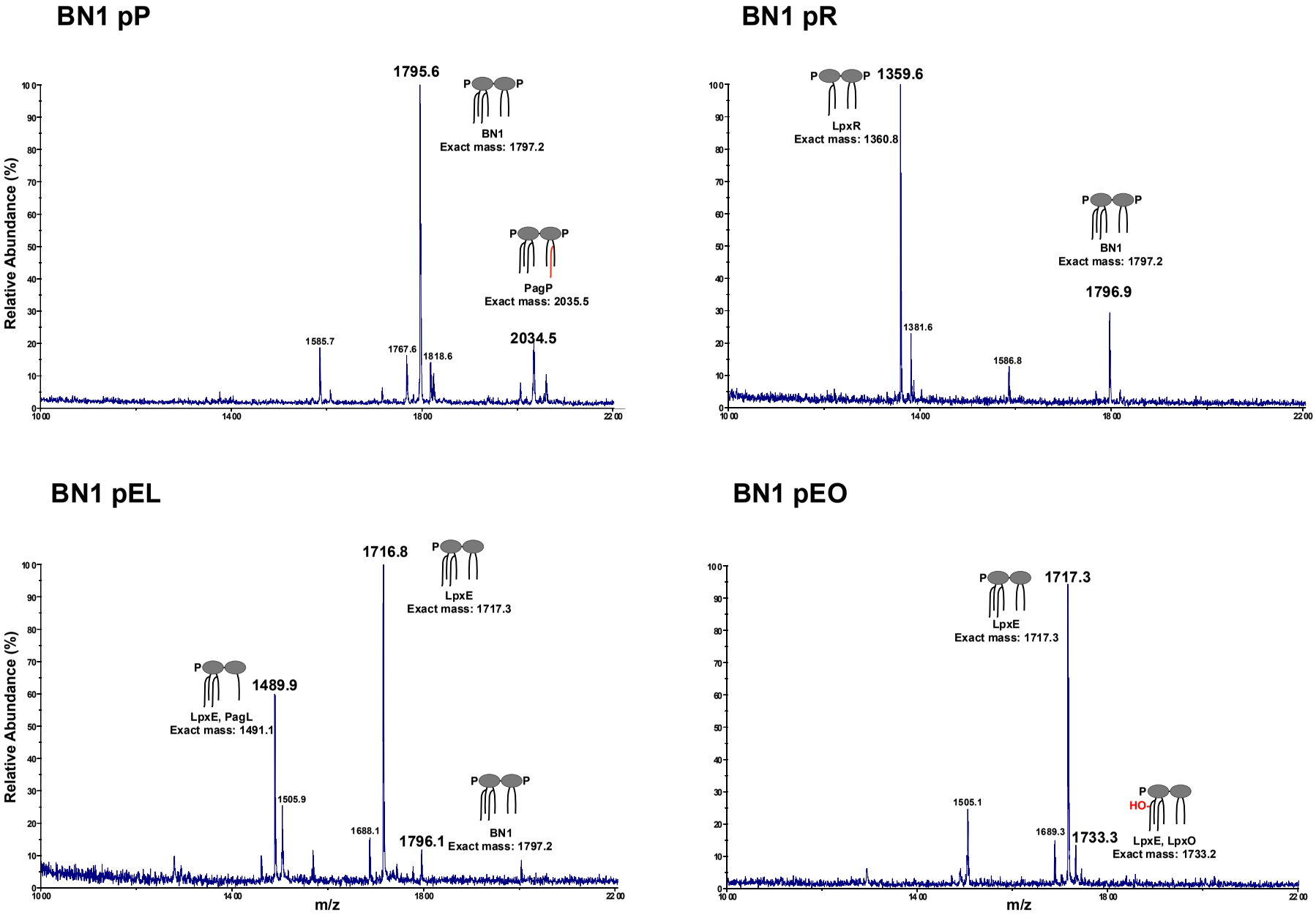
BN1 pP
1795.6
BN1
Exact mass: 1797.2
PagP
Exact mass: 2035.5
2034.5
1585.7
1767.6
1818.6
Relative Abundance (%)
BN1 pR
1359.6
LpxR
Exact mass: 1360.8
BN1
Exact mass: 1797.2
1796.9
1381.6
1586.8
BN1 pEL
1716.8
LpxE
Exact mass: 1717.3
1489.9
LpxE, PagL
Exact mass: 1491.1
1505.9
1688.1
1796.1
BN1
Exact mass: 1797.2
m/z
BN1 pEO
1717.3
LpxE
Exact mass: 1717.3
1505.1
1689.3
1733.3
HO-
LpxE, LpxO
Exact mass: 1733.2
m/z

a, cont'd

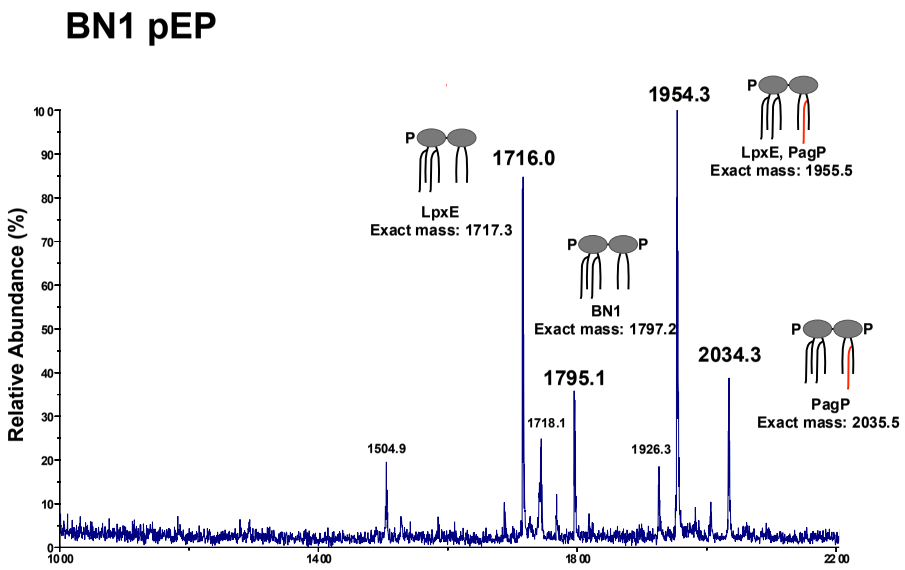
BN1 pEP
Relative Abundance (%)
1954.3
1716.0
LpxE, PagP
Exact mass: 1955.5
LpxE
Exact mass: 1717.3
BN1
Exact mass: 1797.2
2034.3
1795.1
PagP
Exact mass: 2035.5
1718.1
1504.9
1926.3

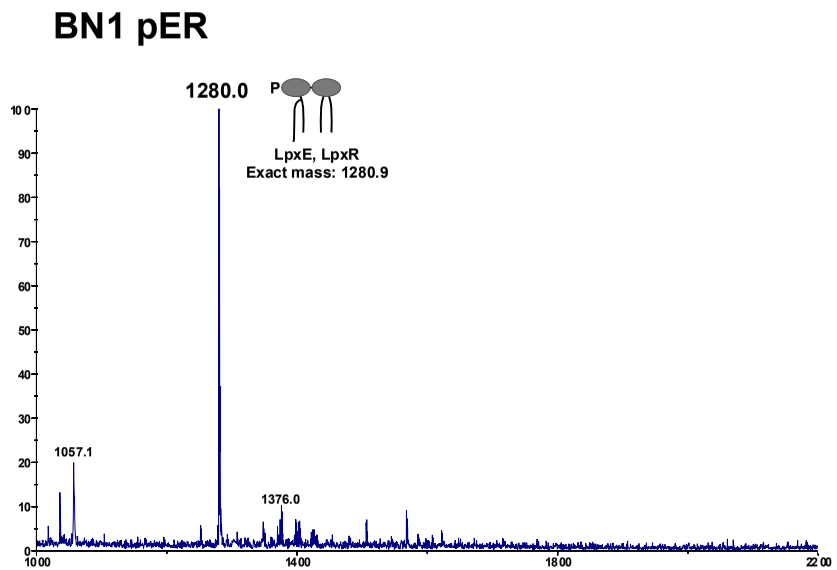
BN1 pER
1280.0
LpxE, LpxR
Exact mass: 1280.9
1057.1
1376.0

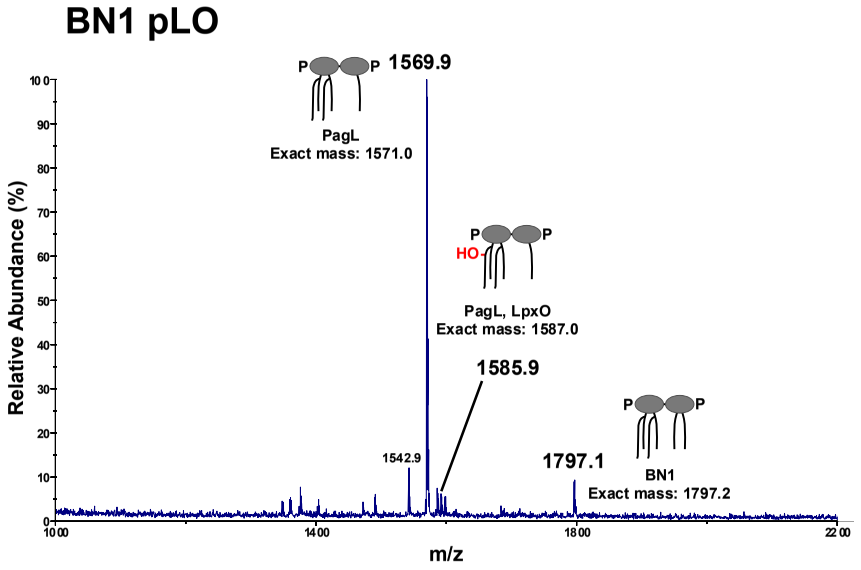
BN1 pLO
Relative Abundance (%)
1569.9
PagL
Exact mass: 1571.0
PagL, LpxO
Exact mass: 1587.0
1585.9
1542.9
1797.1
BN1
Exact mass: 1797.2
m/z

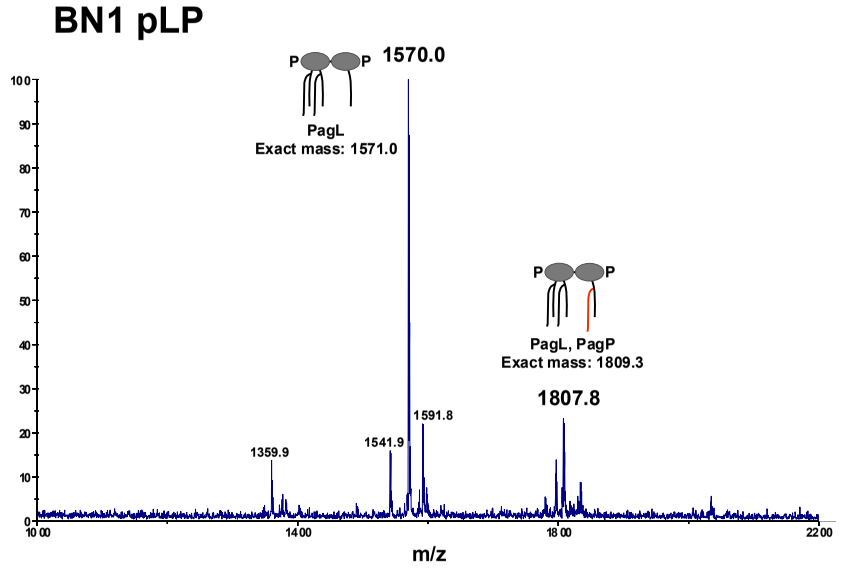
BN1 pLP
1570.0
PagL
Exact mass: 1571.0
PagL, PagP
Exact mass: 1809.3
1807.8
1591.8
1541.9
1359.9
m/z

a, cont'd

BN1 pLR

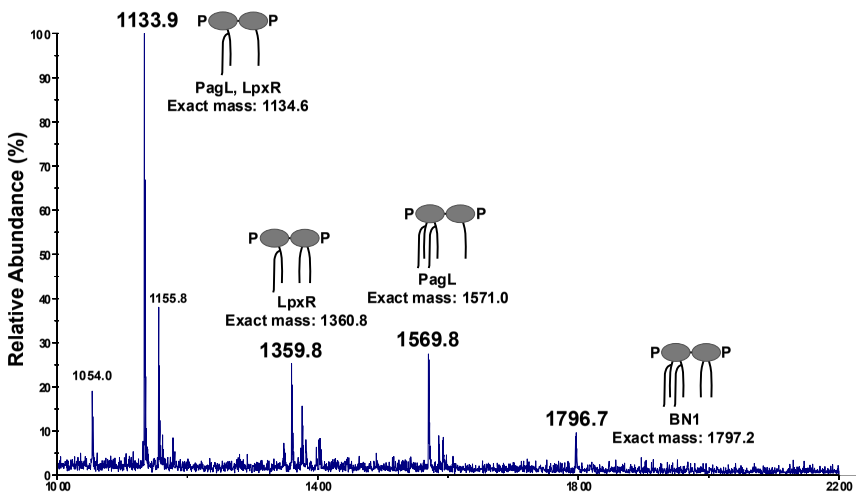

BN1 pOP

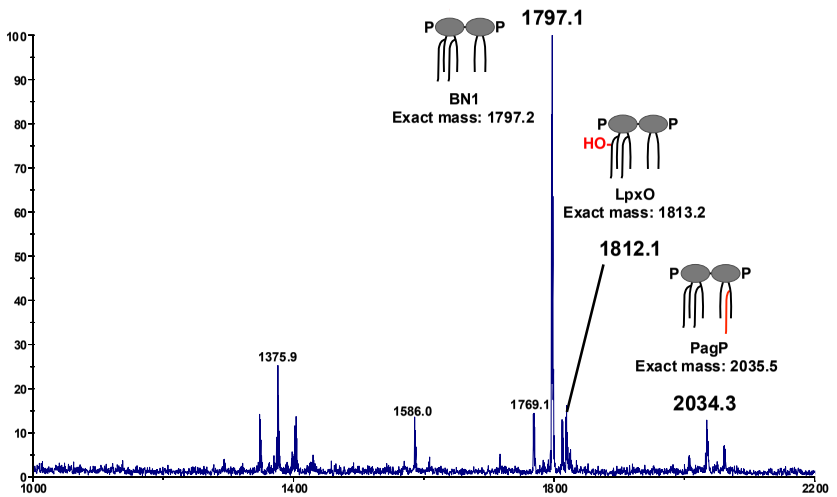

BN1 pOR

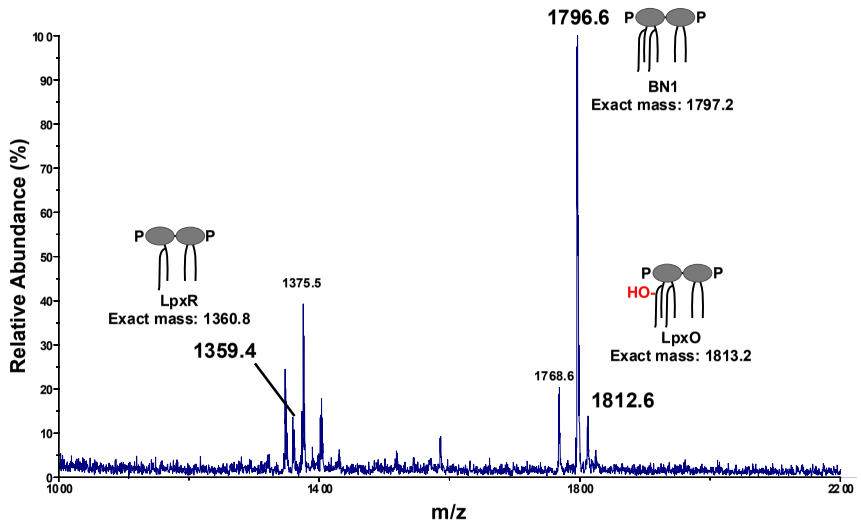

BN1 pPR

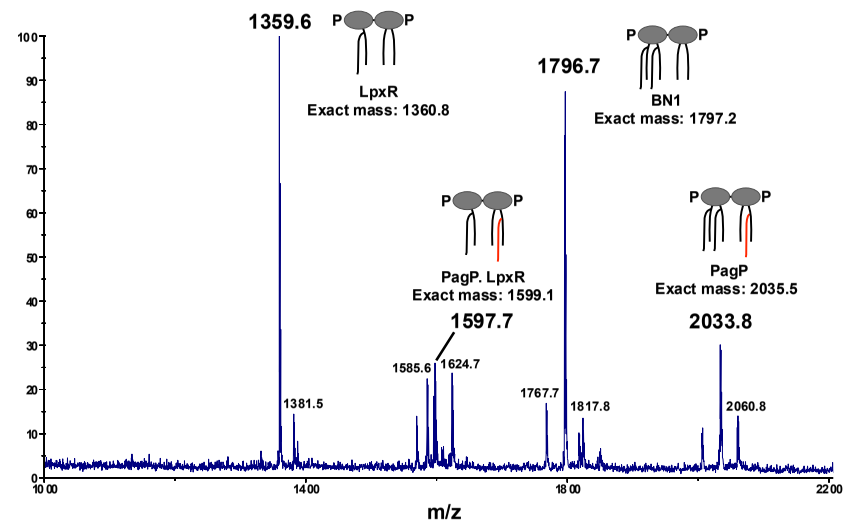

a, cont'd

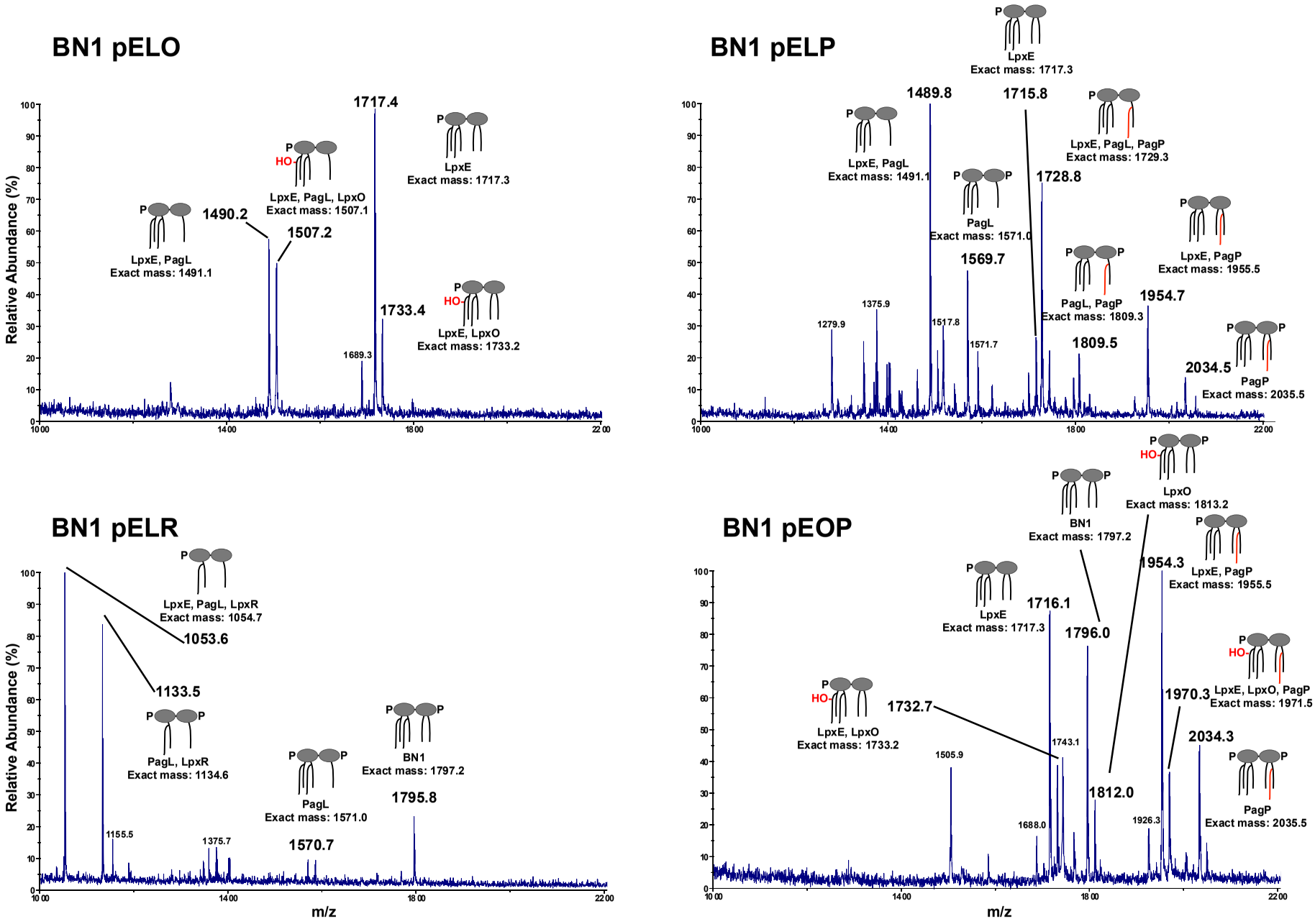
BN1 pELO
Relative Abundance (%)
1717.4
1490.2
1507.2
1733.4
1689.3
LpxE
Exact mass: 1717.3
LpxE, PagL, LpxO
Exact mass: 1507.1
LpxE, PagL
Exact mass: 1491.1
LpxE, LpxO
Exact mass: 1733.2
BN1 pELP
1489.8
1715.8
1728.8
1569.7
1954.7
1809.5
2034.5
1375.9
1279.9
1517.8
1571.7
LpxE, PagL
Exact mass: 1491.1
LpxE, PagL, PagP
Exact mass: 1729.3
PagL
Exact mass: 1571.0
LpxE, PagP
Exact mass: 1955.5
PagL, PagP
Exact mass: 1809.3
PagP
Exact mass: 2035.5
BN1 pELR
1053.6
1133.5
1155.5
1375.7
1570.7
1795.8
LpxE, PagL, LpxR
Exact mass: 1054.7
PagL, LpxR
Exact mass: 1134.6
PagL
Exact mass: 1571.0
BN1
Exact mass: 1797.2
m/z
BN1 pEOP
1716.1
1796.0
1954.3
1732.7
1970.3
2034.3
1743.1
1505.9
1812.0
1688.0
1926.3
LpxO
Exact mass: 1813.2
BN1
Exact mass: 1797.2
LpxE, PagP
Exact mass: 1955.5
LpxE
Exact mass: 1717.3
LpxE, LpxO, PagP
Exact mass: 1971.5
LpxE, LpxO
Exact mass: 1733.2
PagP
Exact mass: 2035.5
m/z

a, cont'd

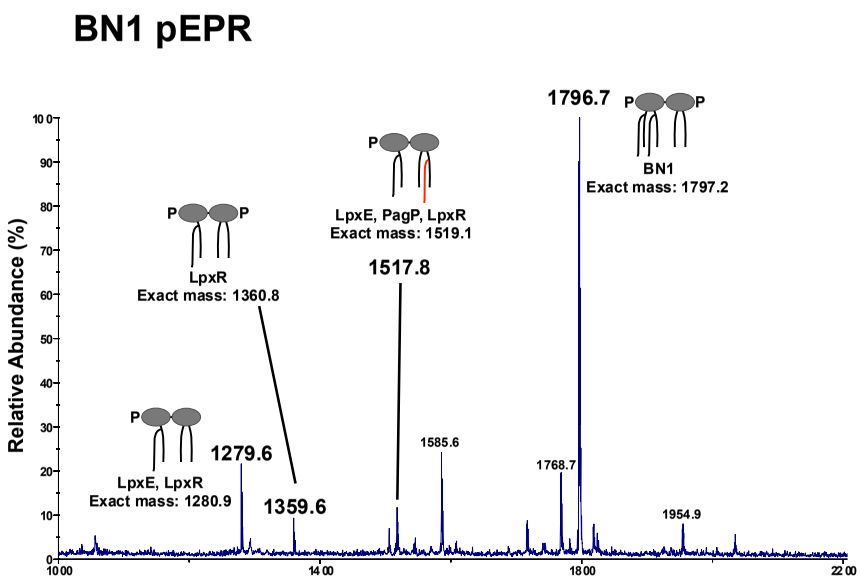
BN1 pEPR
Relative Abundance (%)
1796.7
BN1
Exact mass: 1797.2
LpxE, PagP, LpxR
Exact mass: 1519.1
1517.8
LpxR
Exact mass: 1360.8
LpxE, LpxR
Exact mass: 1280.9
1279.6
1359.6
1585.6
1768.7
1954.9
m/z

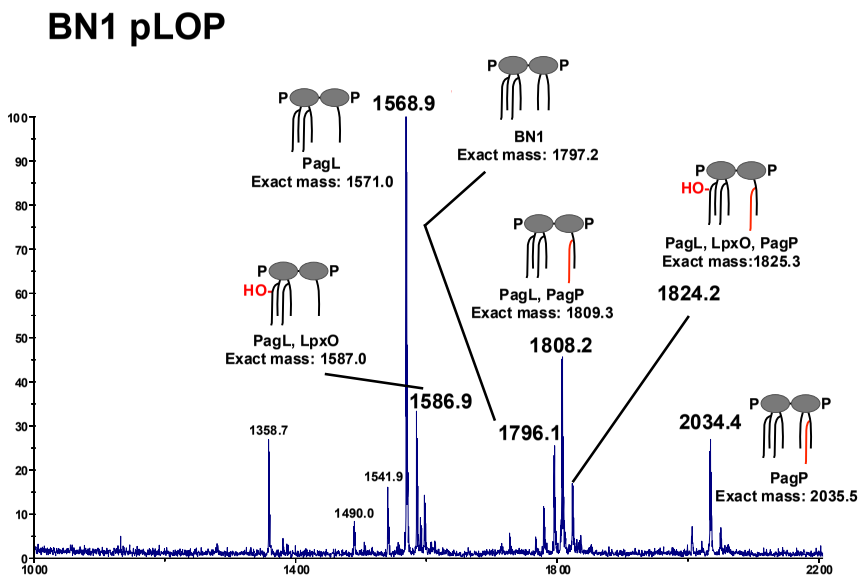
BN1 pLOP
1568.9
PagL
Exact mass: 1571.0
BN1
Exact mass: 1797.2
PagL, LpxO, PagP
Exact mass:1825.3
PagL, PagP
Exact mass: 1809.3
1824.2
PagL, LpxO
Exact mass: 1587.0
1808.2
1586.9
1796.1
2034.4
PagP
Exact mass: 2035.5
1358.7
1541.9
1490.0

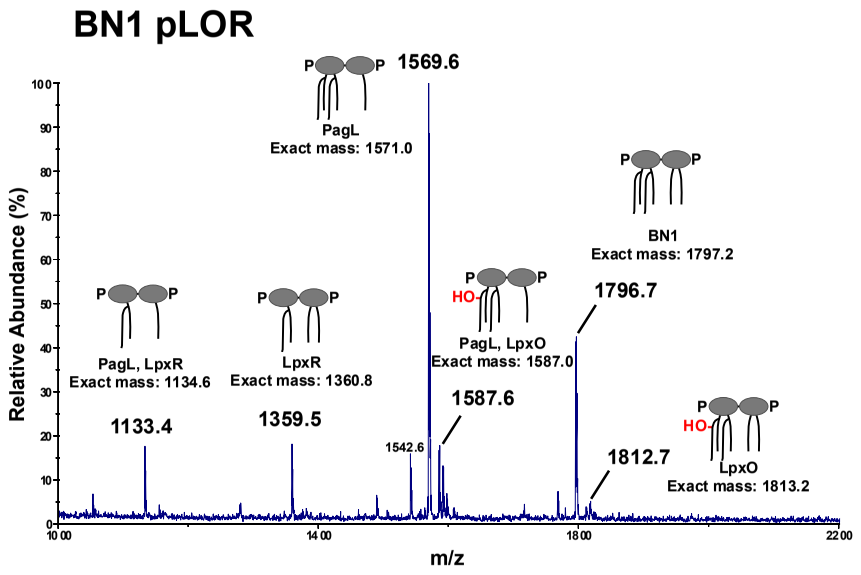
BN1 pLOR
Relative Abundance (%)
1569.6
PagL
Exact mass: 1571.0
BN1
Exact mass: 1797.2
PagL, LpxR
Exact mass: 1134.6
LpxR
Exact mass: 1360.8
PagL, LpxO
Exact mass: 1587.0
1796.7
1133.4
1359.5
1587.6
1542.6
1812.7
LpxO
Exact mass: 1813.2
m/z

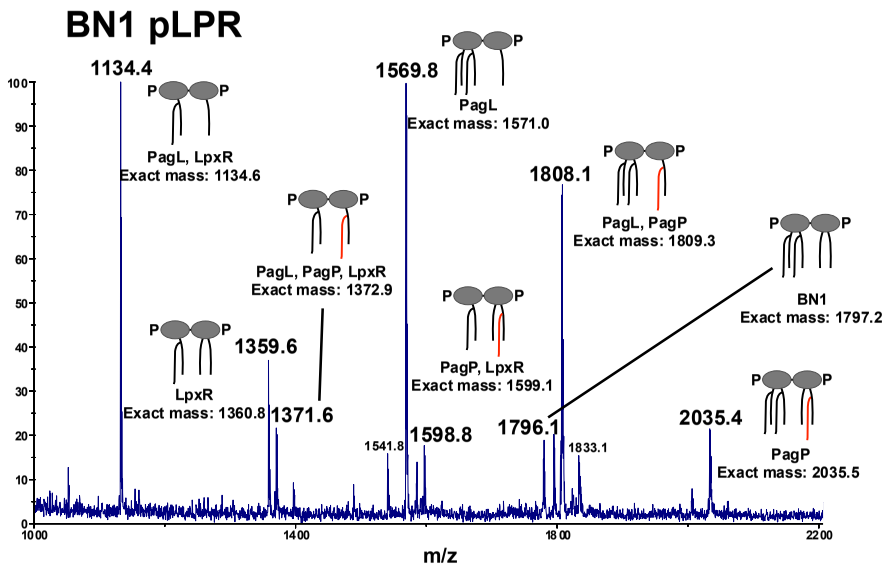
BN1 pLPR
1134.4
1569.8
PagL
Exact mass: 1571.0
PagL, LpxR
Exact mass: 1134.6
1808.1
PagL, PagP
Exact mass: 1809.3
PagL, PagP, LpxR
Exact mass: 1372.9
BN1
Exact mass: 1797.2
1359.6
PagP, LpxR
Exact mass: 1599.1
LpxR
Exact mass: 1360.8
1371.6
1598.8
1796.1
2035.4
PagP
Exact mass: 2035.5
1541.8
1833.1
m/z

a, cont'd

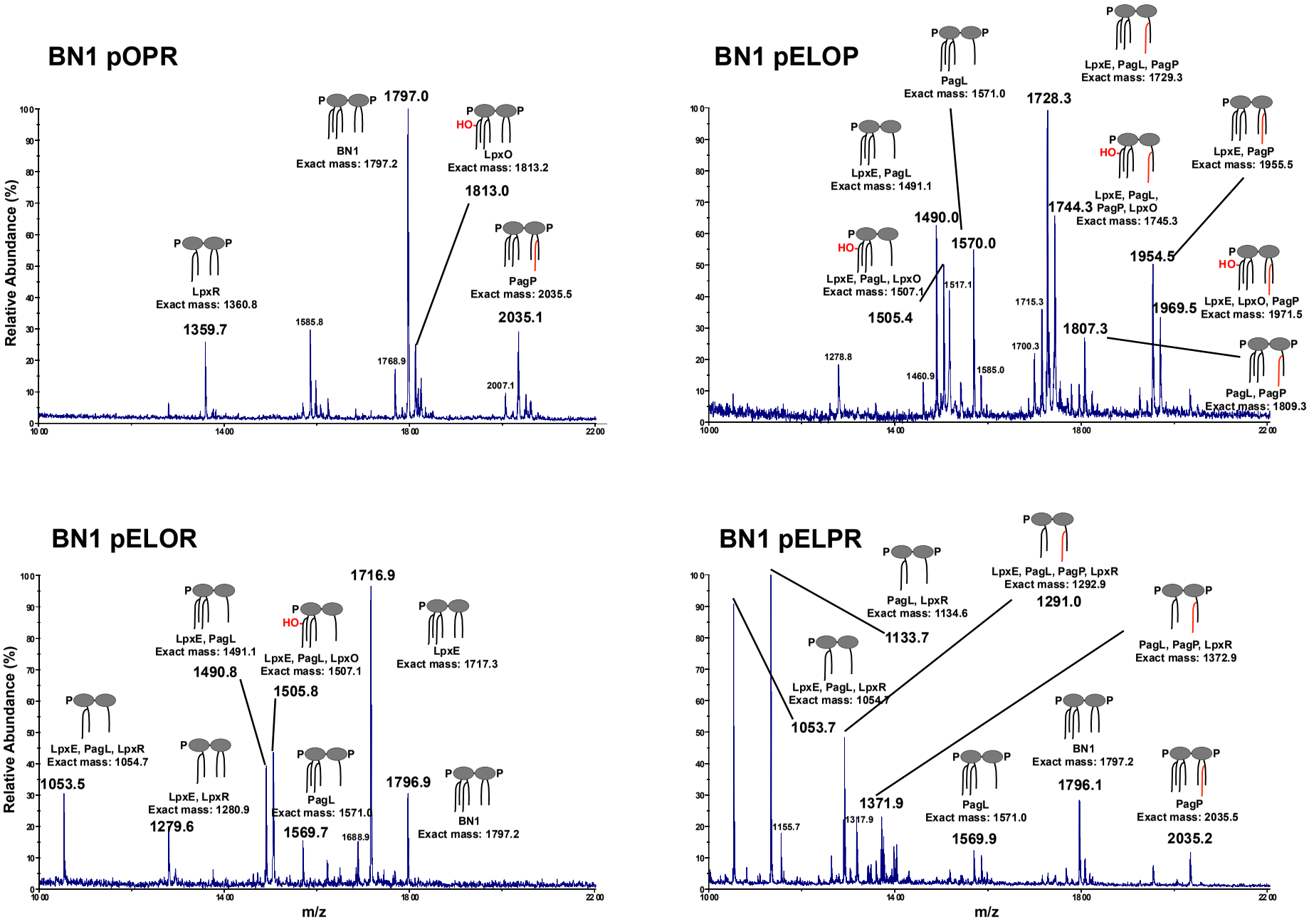
BN1 pOPR
Relative Abundance (%)
BN1
Exact mass: 1797.2
1797.0
LpxO
Exact mass: 1813.2
1813.0
LpxR
Exact mass: 1360.8
1359.7
PagP
Exact mass: 2035.5
2035.1
1585.8
1768.9
2007.1
BN1 pELOP
PagL
Exact mass: 1571.0
LpxE, PagL, PagP
Exact mass: 1729.3
1728.3
LpxE, PagL
Exact mass: 1491.1
LpxE, PagP
Exact mass: 1955.5
LpxE, PagL, PagP, LpxO
Exact mass: 1745.3
1744.3
1490.0
1570.0
1954.5
LpxE, PagL, LpxO
Exact mass: 1507.1
1505.4
LpxE, LpxO, PagP
Exact mass: 1971.5
1969.5
1807.3
PagL, PagP
Exact mass: 1809.3
1517.1
1715.3
1700.3
1278.8
1460.9
1585.0
BN1 pELOR
Relative Abundance (%)
LpxE, PagL
Exact mass: 1491.1
1490.8
LpxE, PagL, LpxO
Exact mass: 1507.1
1505.8
1716.9
LpxE
Exact mass: 1717.3
LpxE, PagL, LpxR
Exact mass: 1054.7
1053.5
LpxE, LpxR
Exact mass: 1280.9
1279.6
PagL
Exact mass: 1571.0
1569.7
1688.9
1796.9
BN1
Exact mass: 1797.2
m/z
BN1 pELPR
PagL, LpxR
Exact mass: 1134.6
1133.7
LpxE, PagL, PagP, LpxR
Exact mass: 1292.9
1291.0
PagL, PagP, LpxR
Exact mass: 1372.9
LpxE, PagL, LpxR
Exact mass: 1054.7
1053.7
BN1
Exact mass: 1797.2
1796.1
1371.9
PagL
Exact mass: 1571.0
1569.9
PagP
Exact mass: 2035.5
2035.2
1155.7
1317.9
m/z

a, cont'd

BN1 pEOPR

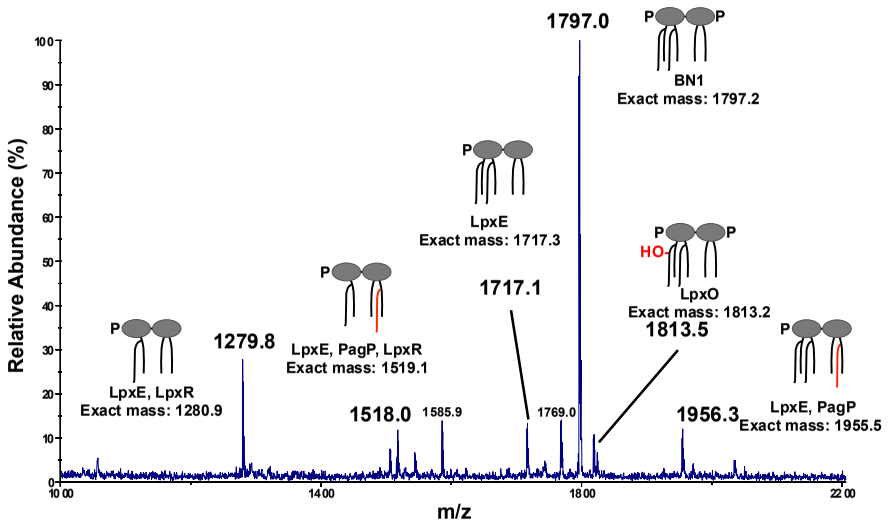

BN1 pLOPR

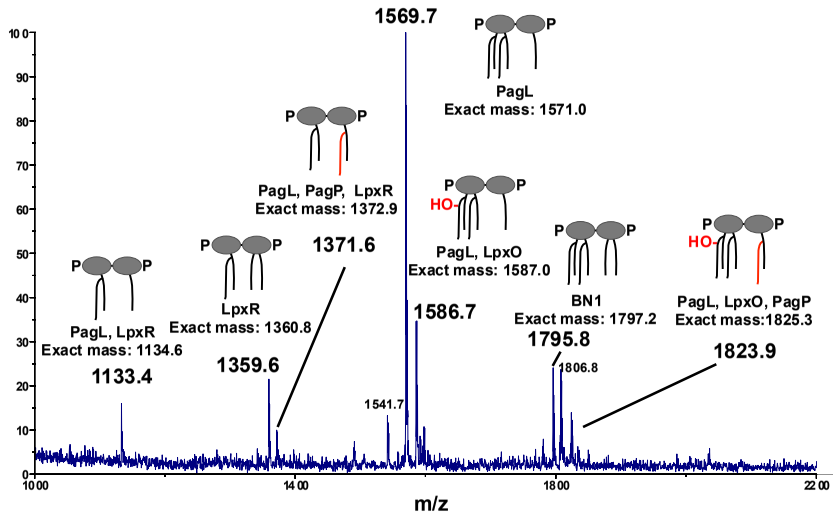

b

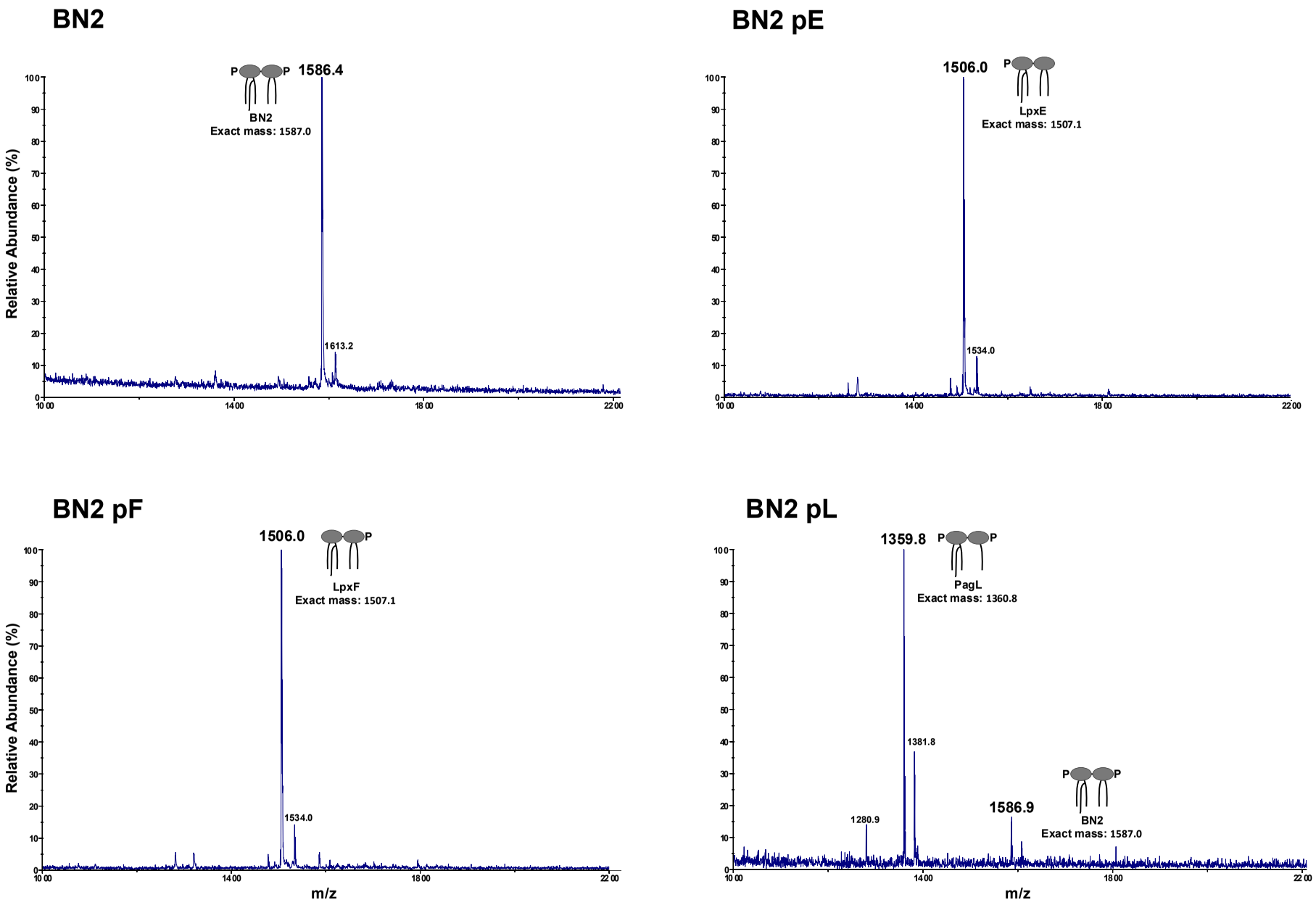
BN2
1586.4
BN2
Exact mass: 1587.0
1613.2
BN2 pE
1506.0
LpxE
Exact mass: 1507.1
1534.0
BN2 pF
1506.0
LpxF
Exact mass: 1507.1
1534.0
BN2 pL
1359.8
PagL
Exact mass: 1360.8
1381.8
1280.9
1586.9
BN2
Exact mass: 1587.0
Relative Abundance (%)
m/z

b, cont'd

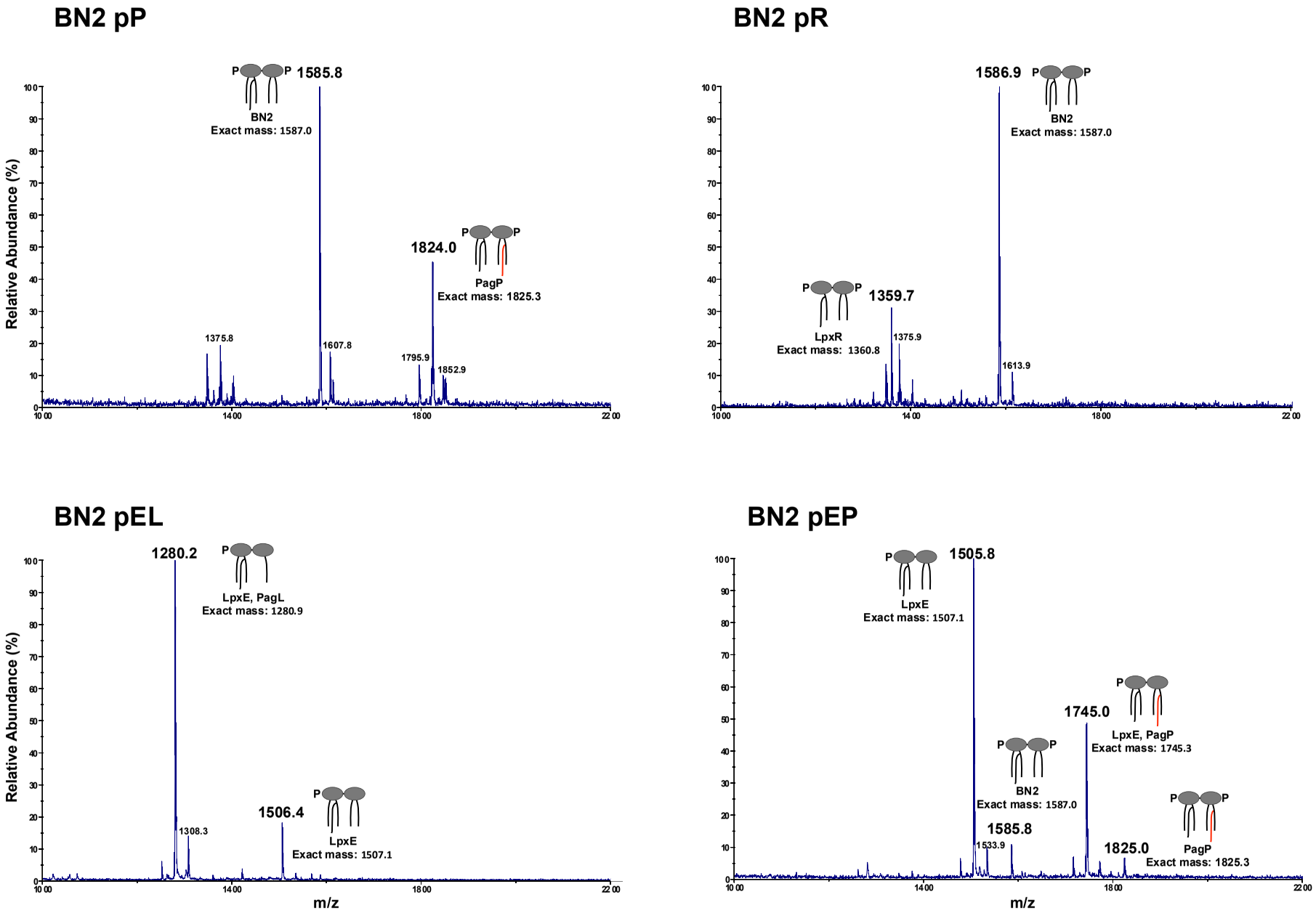
BN2 pP
1585.8
BN2
Exact mass: 1587.0
1824.0
PagP
Exact mass: 1825.3
1375.8
1607.8
1795.9
1852.9
Relative Abundance (%)
BN2 pR
1586.9
BN2
Exact mass: 1587.0
1359.7
LpxR
Exact mass: 1360.8
1375.9
1613.9
BN2 pEL
1280.2
LpxE, PagL
Exact mass: 1280.9
1506.4
LpxE
Exact mass: 1507.1
1308.3
Relative Abundance (%)
m/z
BN2 pEP
1505.8
LpxE
Exact mass: 1507.1
1745.0
LpxE, PagP
Exact mass: 1745.3
BN2
Exact mass: 1587.0
1585.8
1533.9
1825.0
PagP
Exact mass: 1825.3
m/z

b, cont'd

BN2 pER

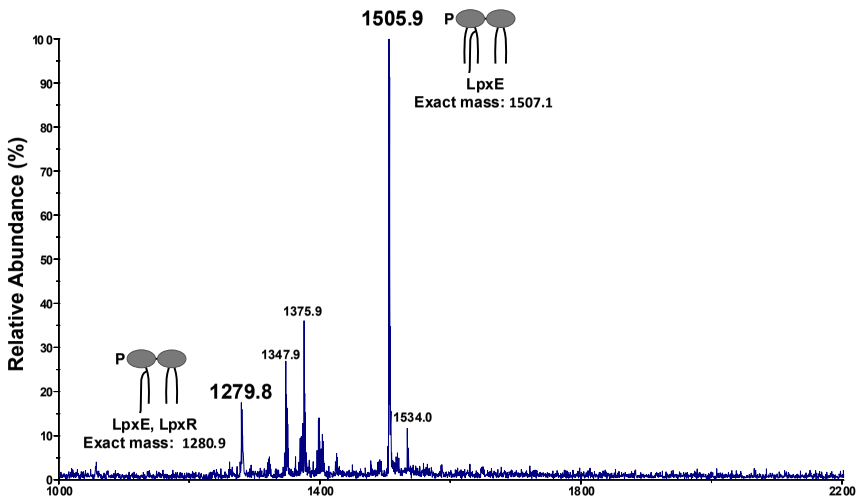

BN2 pFL

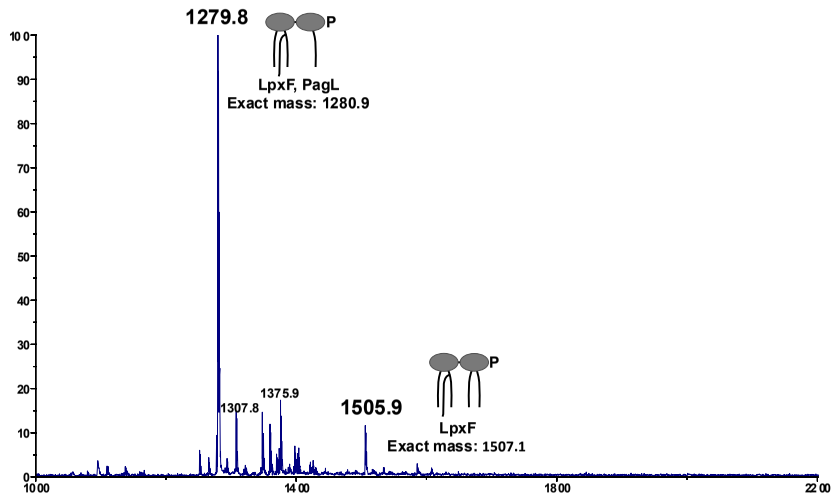

BN2 pFP

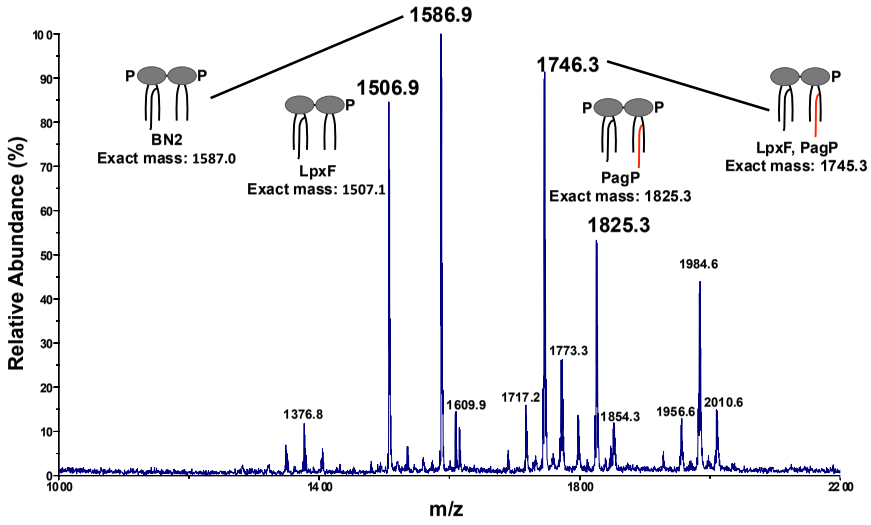

BN2 pFR

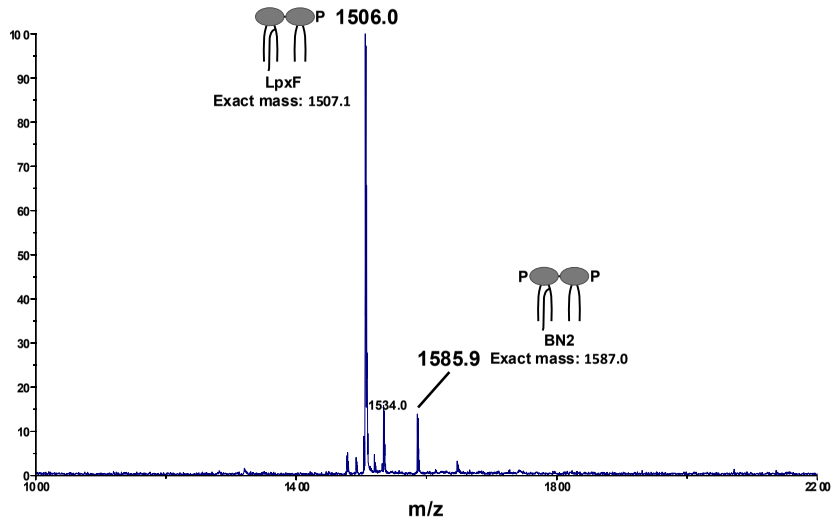

b, cont'd

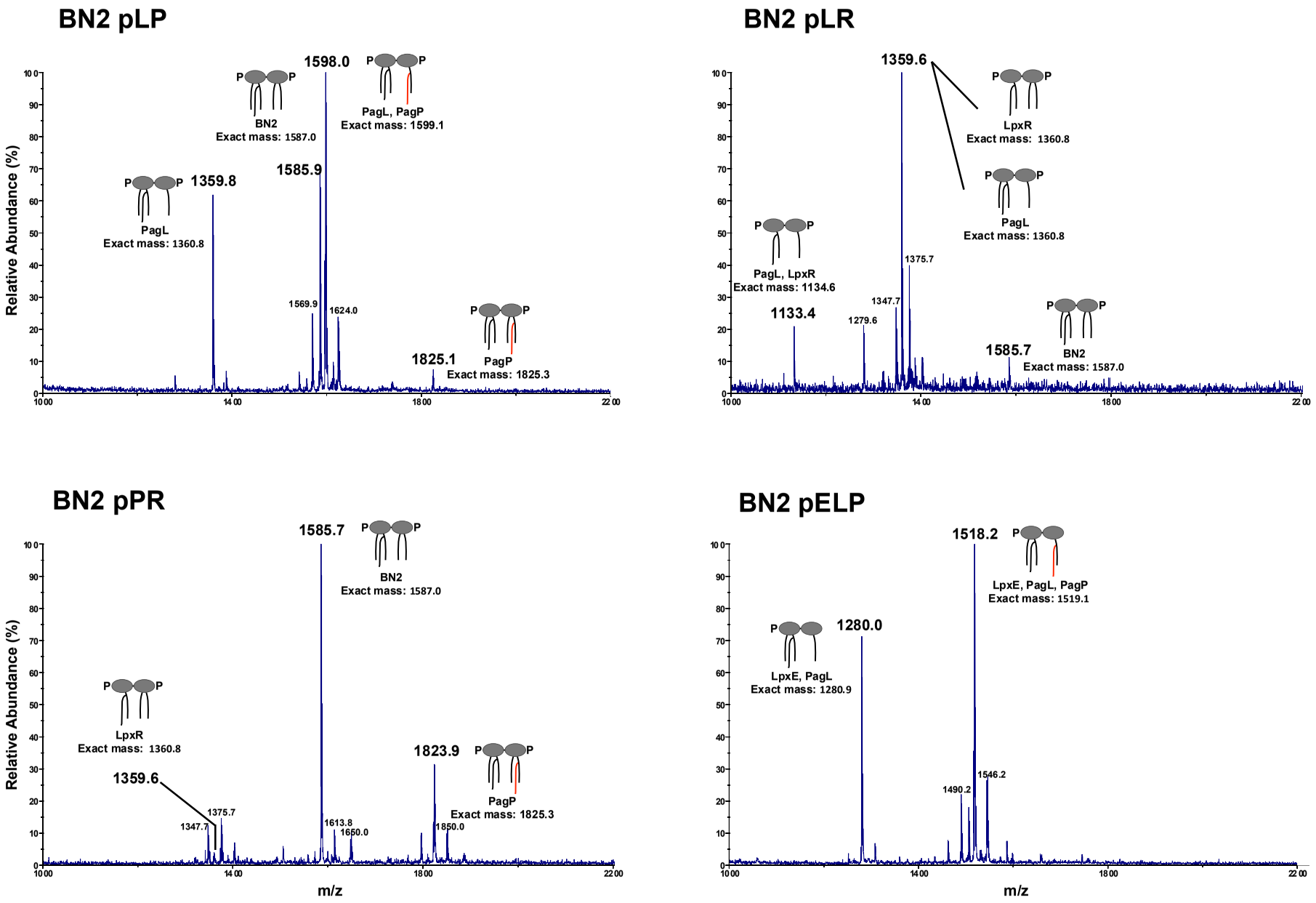
BN2 pLP
1598.0
BN2
Exact mass: 1587.0
PagL, PagP
Exact mass: 1599.1
1585.9
1359.8
PagL
Exact mass: 1360.8
1569.9
1624.0
1825.1
PagP
Exact mass: 1825.3
Relative Abundance (%)
BN2 pLR
1359.6
LpxR
Exact mass: 1360.8
PagL
Exact mass: 1360.8
PagL, LpxR
Exact mass: 1134.6
1375.7
1347.7
1279.6
1133.4
1585.7
BN2
Exact mass: 1587.0
BN2 pPR
1585.7
BN2
Exact mass: 1587.0
LpxR
Exact mass: 1360.8
1823.9
PagP
Exact mass: 1825.3
1359.6
1375.7
1347.7
1613.8
1650.0
1850.0
Relative Abundance (%)
m/z
BN2 pELP
1518.2
LpxE, PagL, PagP
Exact mass: 1519.1
1280.0
LpxE, PagL
Exact mass: 1280.9
1546.2
1490.2
m/z

b, cont'd

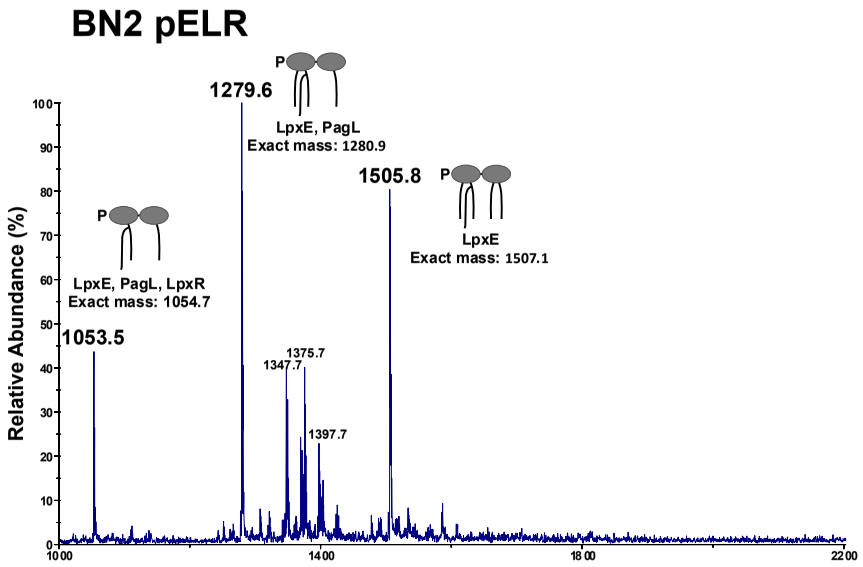
BN2 pELR
Relative Abundance (%)
1279.6
LpxE, PagL
Exact mass: 1280.9
1505.8
LpxE
Exact mass: 1507.1
LpxE, PagL, LpxR
Exact mass: 1054.7
1053.5
1375.7
1347.7
1397.7

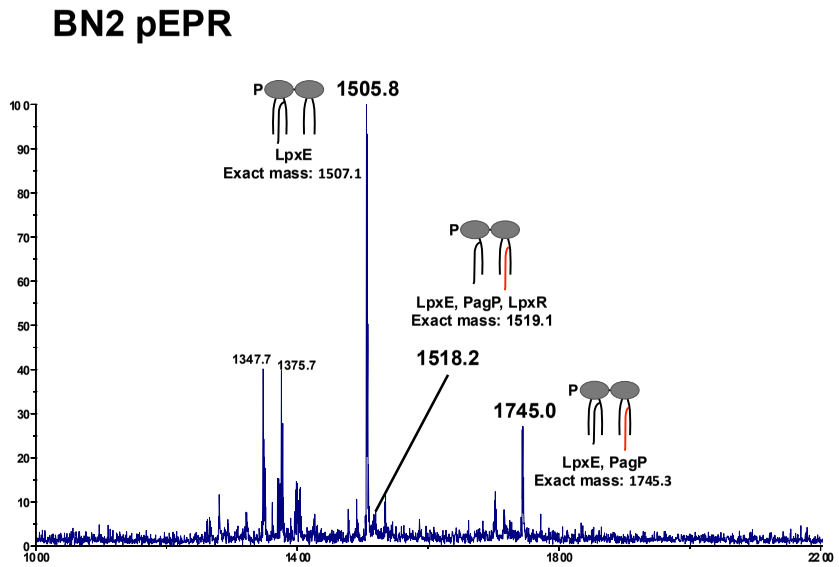
BN2 pEPR
1505.8
LpxE
Exact mass: 1507.1
LpxE, PagP, LpxR
Exact mass: 1519.1
1347.7
1375.7
1518.2
1745.0
LpxE, PagP
Exact mass: 1745.3

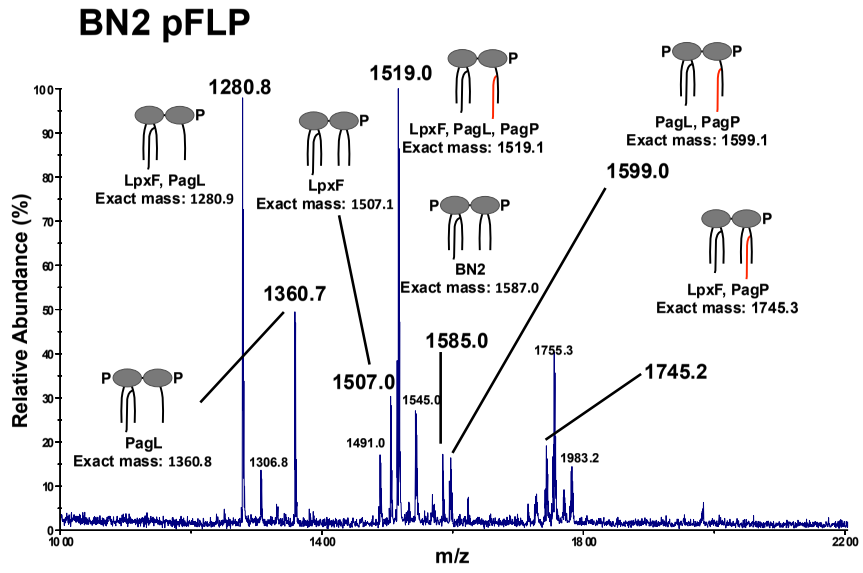
BN2 pFLP
Relative Abundance (%)
1280.8
LpxF, PagL
Exact mass: 1280.9
1519.0
LpxF, PagL, PagP
Exact mass: 1519.1
PagL, PagP
Exact mass: 1599.1
LpxF
Exact mass: 1507.1
1599.0
BN2
Exact mass: 1587.0
LpxF, PagP
Exact mass: 1745.3
1360.7
1585.0
1755.3
1507.0
1745.2
1545.0
1491.0
1983.2
PagL
Exact mass: 1360.8
1306.8
m/z

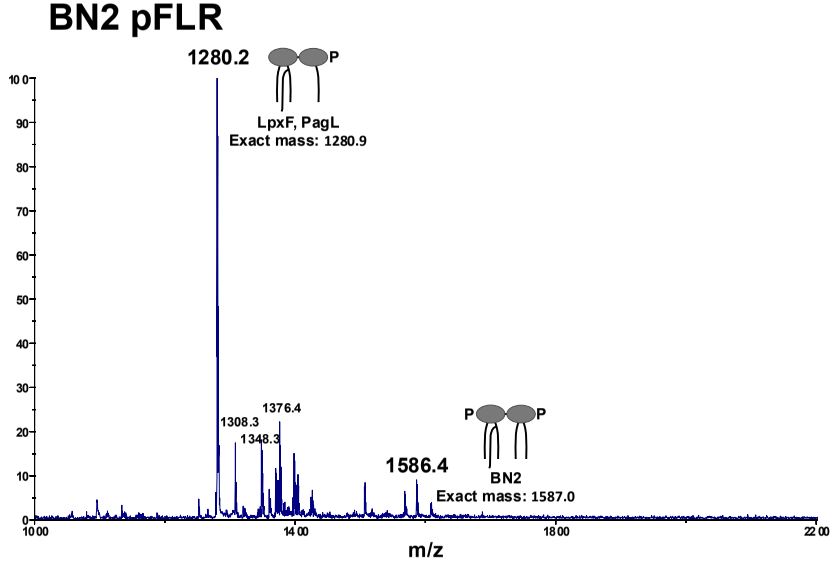
BN2 pFLR
1280.2
LpxF, PagL
Exact mass: 1280.9
1376.4
1308.3
1348.3
1586.4
BN2
Exact mass: 1587.0
m/z

b, cont'd

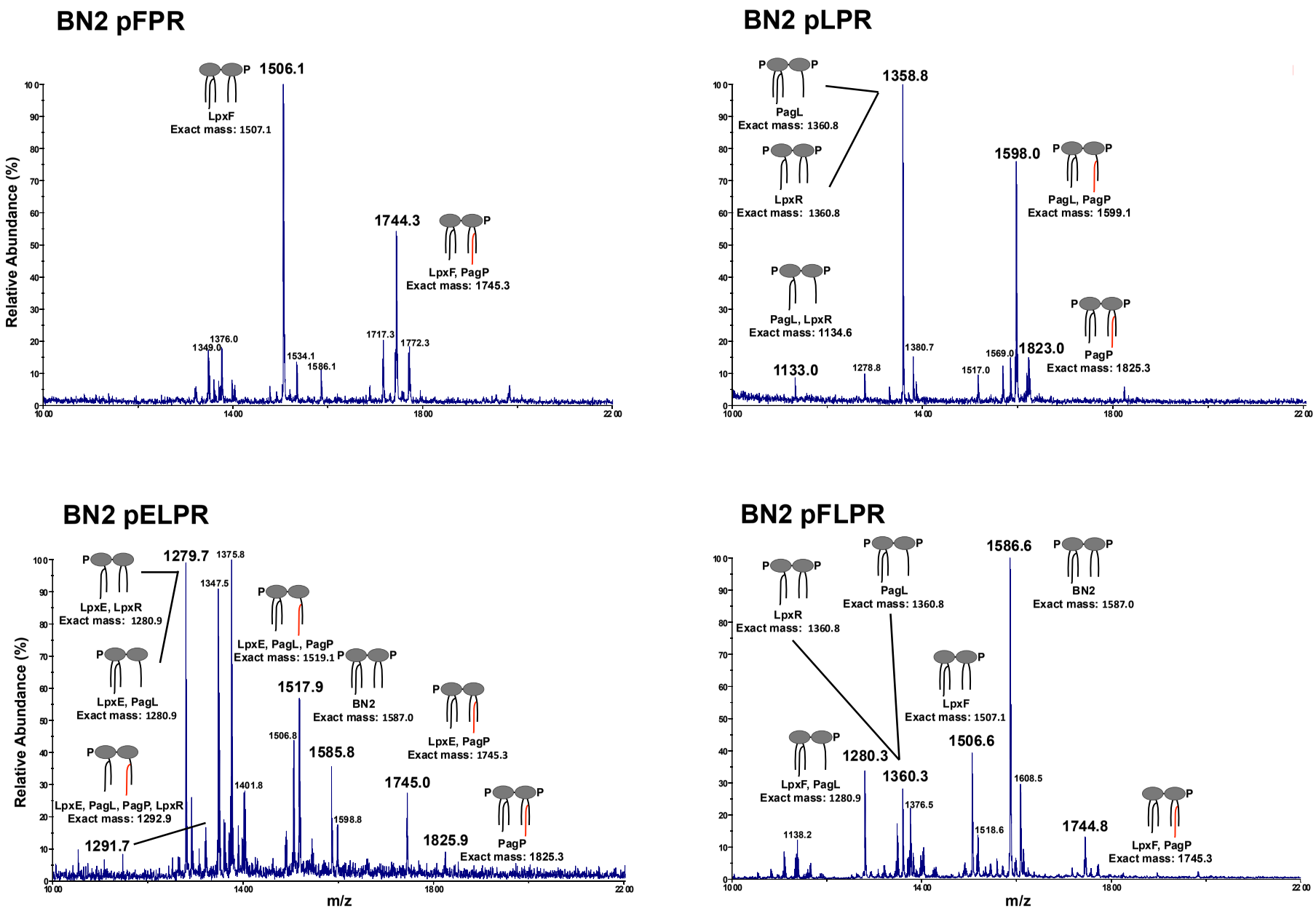
BN2 pFPR
1506.1
LpxF
Exact mass: 1507.1
1744.3
LpxF, PagP
Exact mass: 1745.3
Relative Abundance (%)
BN2 pLPR
1358.8
PagL
Exact mass: 1360.8
LpxR
Exact mass: 1360.8
1598.0
PagL, PagP
Exact mass: 1599.1
PagL, LpxR
Exact mass: 1134.6
1823.0
PagP
Exact mass: 1825.3
BN2 pELPR
1279.7
LpxE, LpxR
Exact mass: 1280.9
LpxE, PagL
Exact mass: 1280.9
LpxE, PagL, PagP
Exact mass: 1519.1
1517.9
BN2
Exact mass: 1587.0
LpxE, PagP
Exact mass: 1745.3
LpxE, PagL, PagP, LpxR
Exact mass: 1292.9
1585.8
1745.0
1291.7
1825.9
PagP
Exact mass: 1825.3
m/z
BN2 pFLPR
1586.6
LpxR
Exact mass: 1360.8
PagL
Exact mass: 1360.8
BN2
Exact mass: 1587.0
LpxF
Exact mass: 1507.1
LpxF, PagL
Exact mass: 1280.9
1280.3
1360.3
1506.6
1744.8
LpxF, PagP
Exact mass: 1745.3
m/z

c

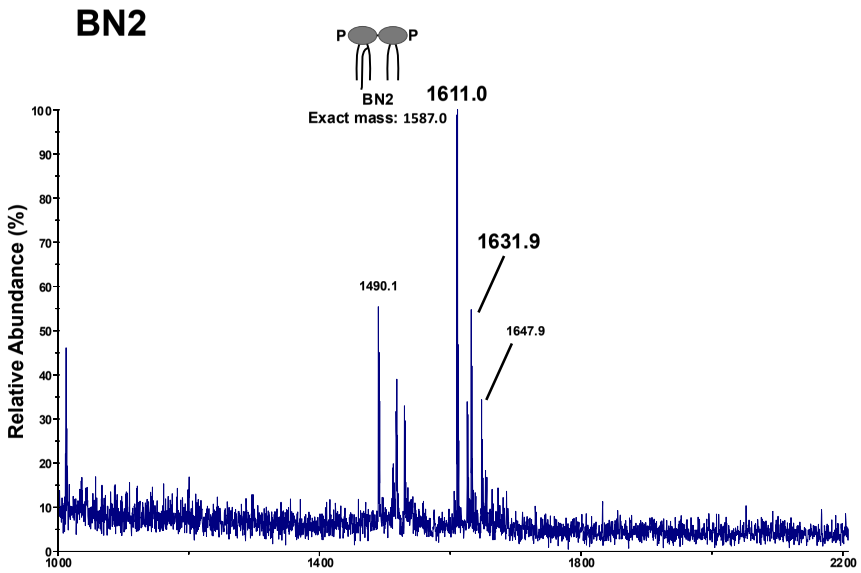
BN2
P
P
BN2
Exact mass: 1587.0
1611.0
1631.9
1490.1
1647.9
Relative Abundance (%)

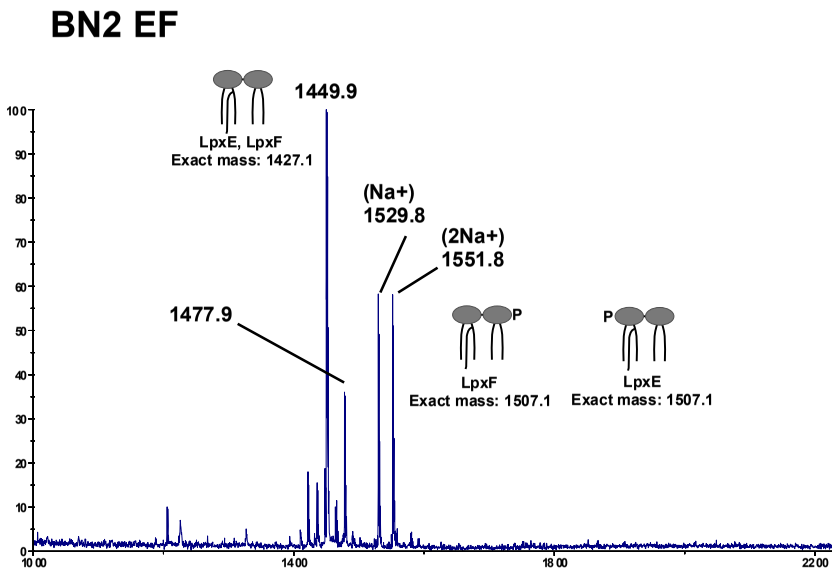
BN2 EF
1449.9
LpxE, LpxF
Exact mass: 1427.1
(Na+)
1529.8
(2Na+)
1551.8
1477.9
P
P
LpxF
Exact mass: 1507.1
P
LpxE
Exact mass: 1507.1

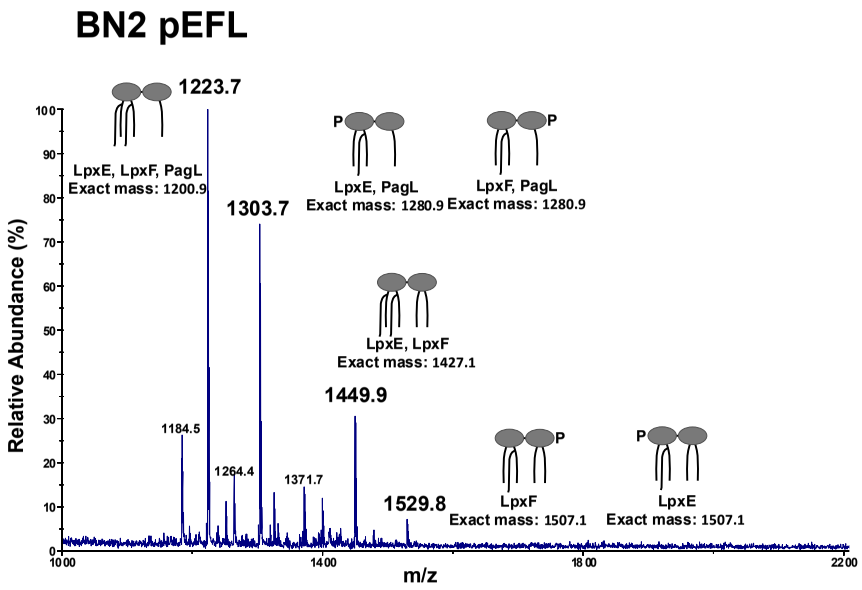
BN2 pEFL
1223.7
LpxE, LpxF, PagL
Exact mass: 1200.9
P
P
LpxE, PagL
Exact mass: 1280.9
LpxF, PagL
Exact mass: 1280.9
1303.7
LpxE, LpxF
Exact mass: 1427.1
1449.9
1184.5
1264.4
1371.7
1529.8
P
LpxF
Exact mass: 1507.1
P
LpxE
Exact mass: 1507.1
Relative Abundance (%)
m/z

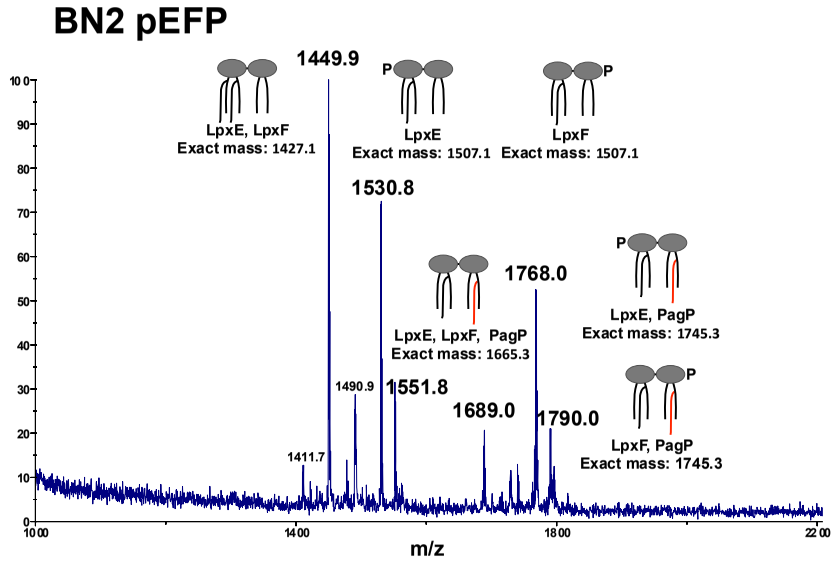
BN2 pEFP
1449.9
LpxE, LpxF
Exact mass: 1427.1
P
P
LpxE
Exact mass: 1507.1
LpxF
Exact mass: 1507.1
1530.8
1768.0
P
LpxE, PagP
Exact mass: 1745.3
LpxE, LpxF, PagP
Exact mass: 1665.3
1490.9
1551.8
1689.0
1790.0
1411.7
P
LpxF, PagP
Exact mass: 1745.3
m/z

c, cont'd

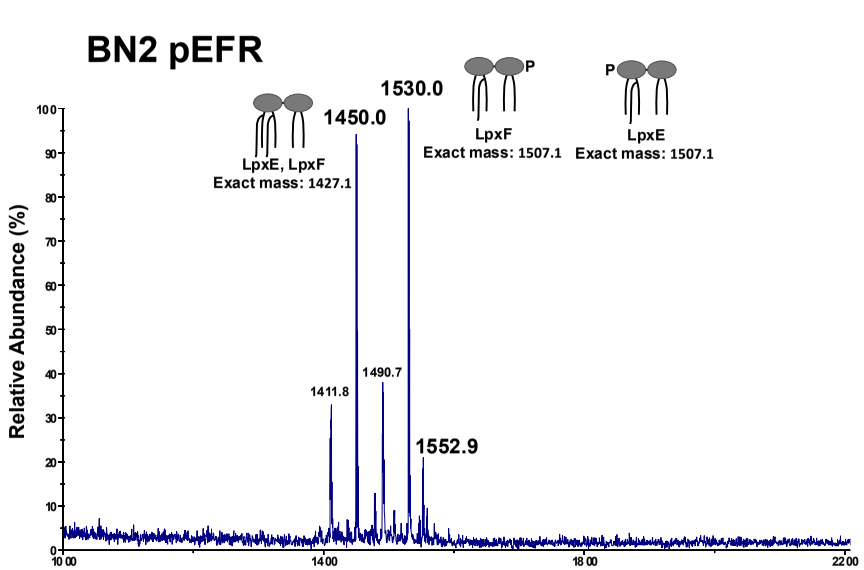
BN2 pEFR
Relative Abundance (%)
1530.0
1450.0
LpxE, LpxF
Exact mass: 1427.1
LpxF
Exact mass: 1507.1
LpxE
Exact mass: 1507.1
1411.8
1490.7
1552.9
m/z

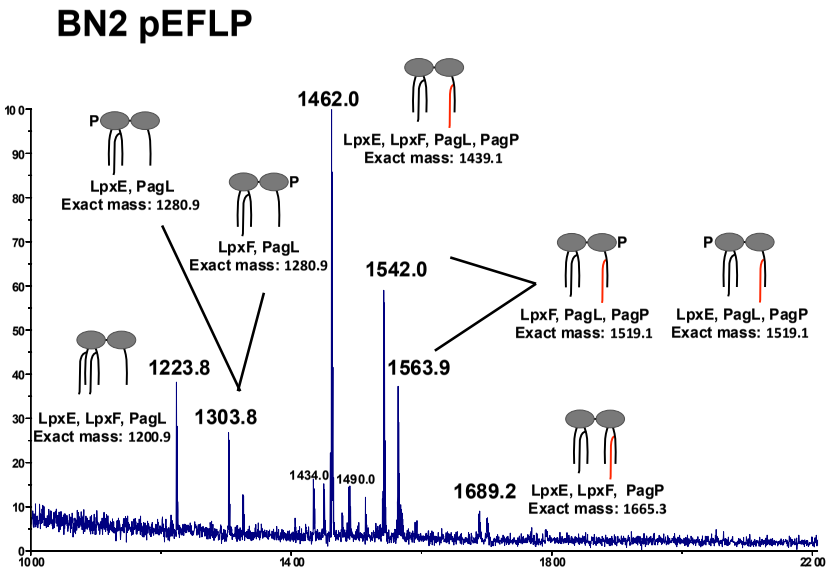
BN2 pEFLP
1462.0
LpxE, LpxF, PagL, PagP
Exact mass: 1439.1
LpxE, PagL
Exact mass: 1280.9
LpxF, PagL
Exact mass: 1280.9
1542.0
LpxF, PagL, PagP
Exact mass: 1519.1
LpxE, PagL, PagP
Exact mass: 1519.1
1223.8
1563.9
LpxE, LpxF, PagL
Exact mass: 1200.9
1303.8
1434.0
1490.0
1689.2
LpxE, LpxF, PagP
Exact mass: 1665.3
m/z

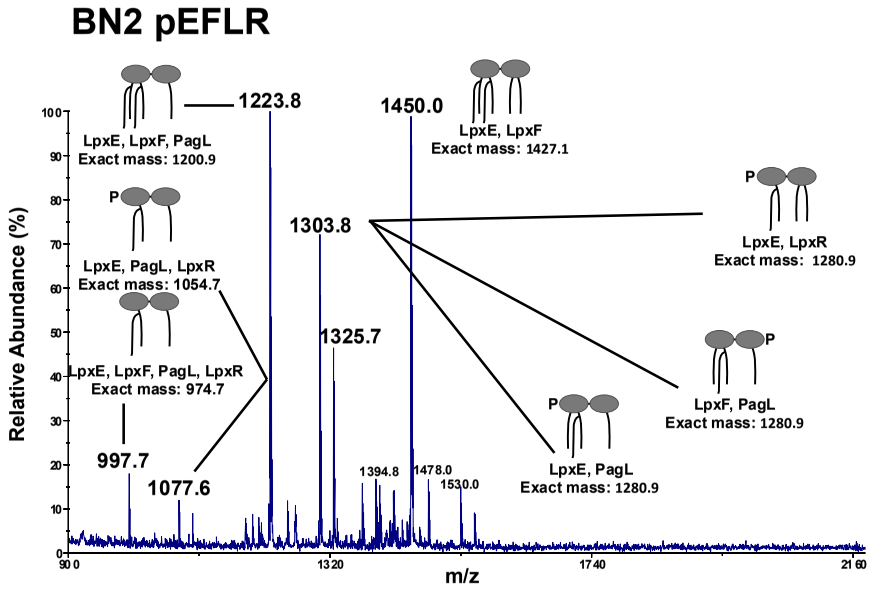
BN2 pEFLR
Relative Abundance (%)
1223.8
1450.0
LpxE, LpxF
Exact mass: 1427.1
LpxE, LpxF, PagL
Exact mass: 1200.9
LpxE, PagL, LpxR
Exact mass: 1054.7
1303.8
LpxE, LpxR
Exact mass: 1280.9
1325.7
LpxE, LpxF, PagL, LpxR
Exact mass: 974.7
LpxF, PagL
Exact mass: 1280.9
997.7
1077.6
LpxE, PagL
Exact mass: 1280.9
1394.8
1478.0
1530.0
m/z

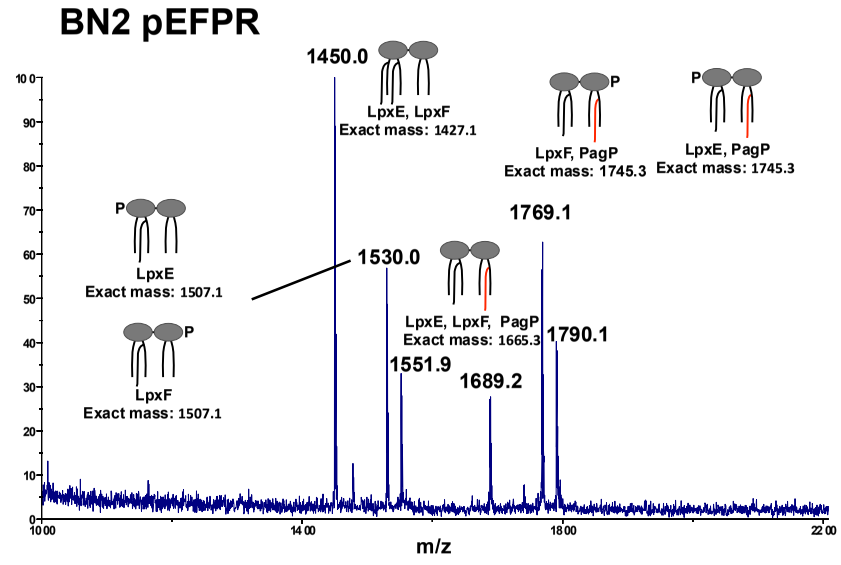
BN2 pEFPR
1450.0
LpxE, LpxF
Exact mass: 1427.1
LpxF, PagP
Exact mass: 1745.3
LpxE, PagP
Exact mass: 1745.3
1769.1
LpxE
Exact mass: 1507.1
1530.0
LpxE, LpxF, PagP
Exact mass: 1665.3
1790.1
1551.9
1689.2
LpxF
Exact mass: 1507.1
m/z

Fig. S3. Mass spectra of combinatorial strains. All spectra, excluding the 3 examples presented in the main text, can be found in this figure. Lipid A structures corresponding to the mass peak are depicted by cartoons next to the peak. Peak clusters at *m/z* ~1375 correspond to phospholipid contamination, confirmed by TLC isolation of the species. The labile 1-phosphate can be lost, resulting in a mass difference of ~ 80 mass units. a,b) Negative ion mode MS of BN1 and BN2 strains, respectively, confirmed the activity of the enzymes expressed in combinations. A minor species of penta-acylated lipid A can be observed in some enzyme combinations, corresponding to a peak at *m/z* ~1585. c) Positive ion mode MS was done for all strains expressing both phosphatases, LpxE and LpxF. Positive mode often results in single or double sodium adducts on the molecules, resulting in peak masses that are ~23 or 46 mass units higher than the exact mass of each structure.

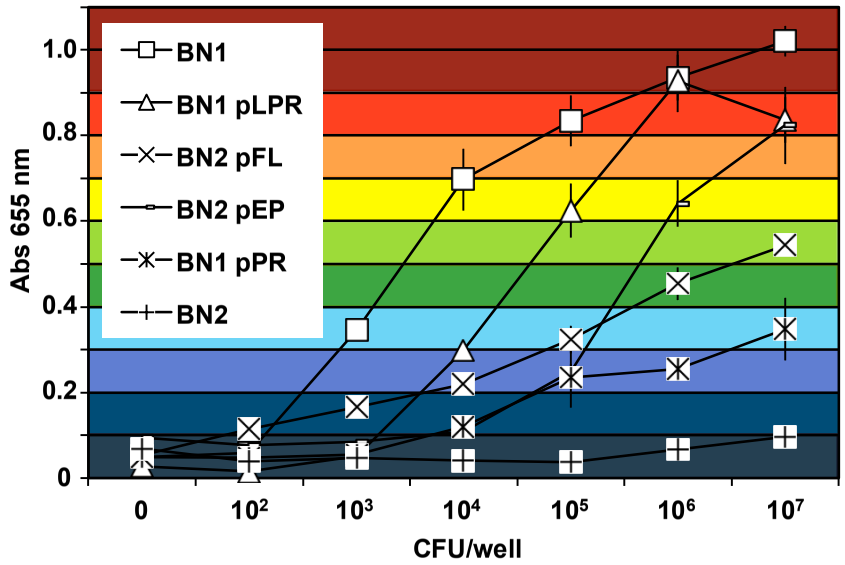

Fig. S4. Colorimetric designations based on TLR4 stimulation by BN1. Selected samples are shown in the graph to illustrate the range of TLR4 stimulation that results from incubation of whole bacteria cells with HEK-Blue cells expressing TLR4, MD-2 and CD14. Color scale is based on the stimulation curve of the BN1 sample and represents the delineations of the colorimetric scale used in Fig. 2c,d.

Fig S5, a

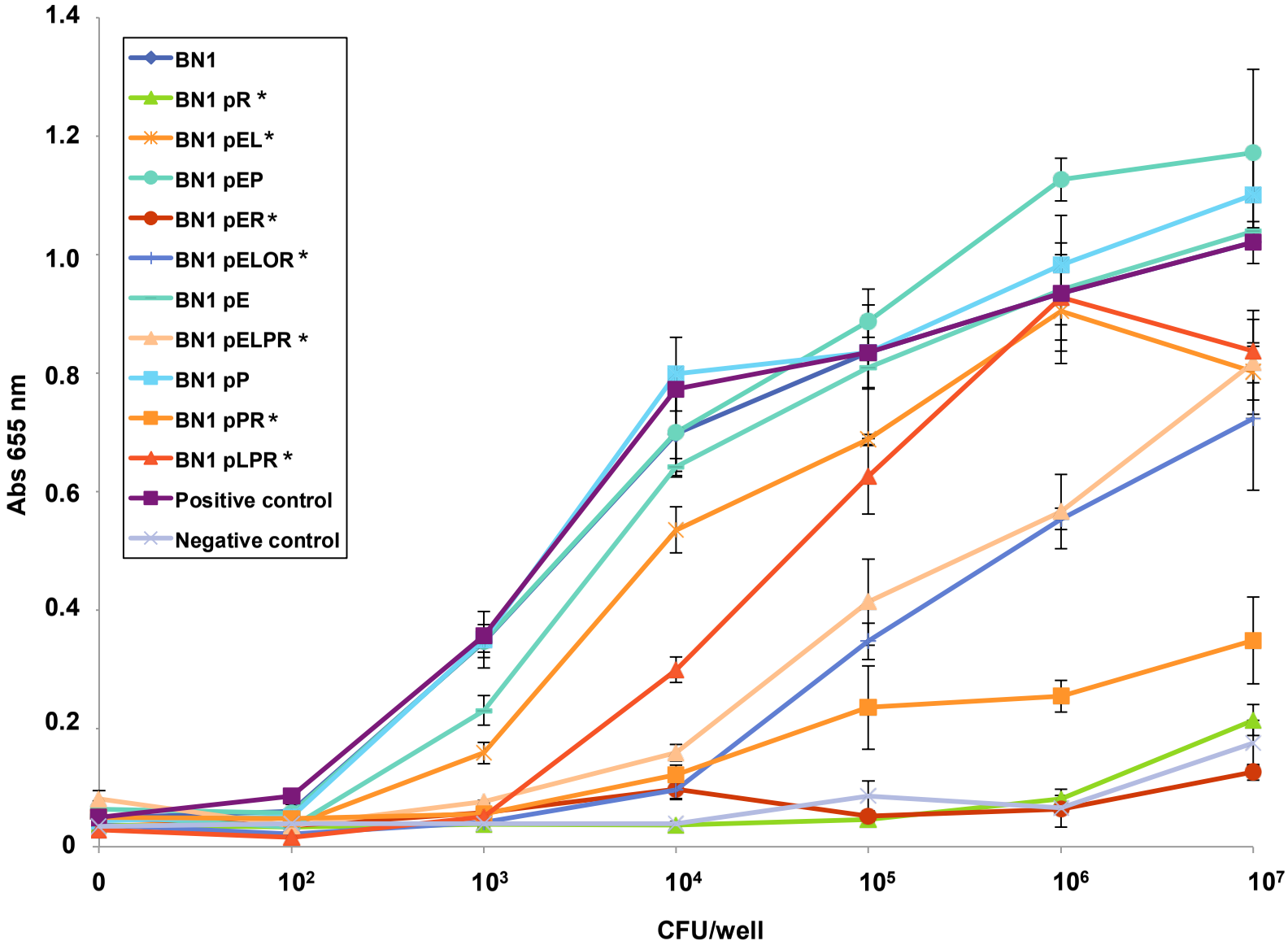
1.4
1.2
1.0
0.8
0.6
0.4
0.2
0
Abs 655 nm
BN1
BN1 pR *
BN1 pEL*
BN1 pEP
BN1 pER*
BN1 pELOR*
BN1 pE
BN1 pELPR *
BN1 pP
BN1 pPR*
BN1 pLPR *
Positive control
Negative control
0
10²
10³
10⁴
10⁵
10⁶
10⁷
CFU/well

a, cont'd

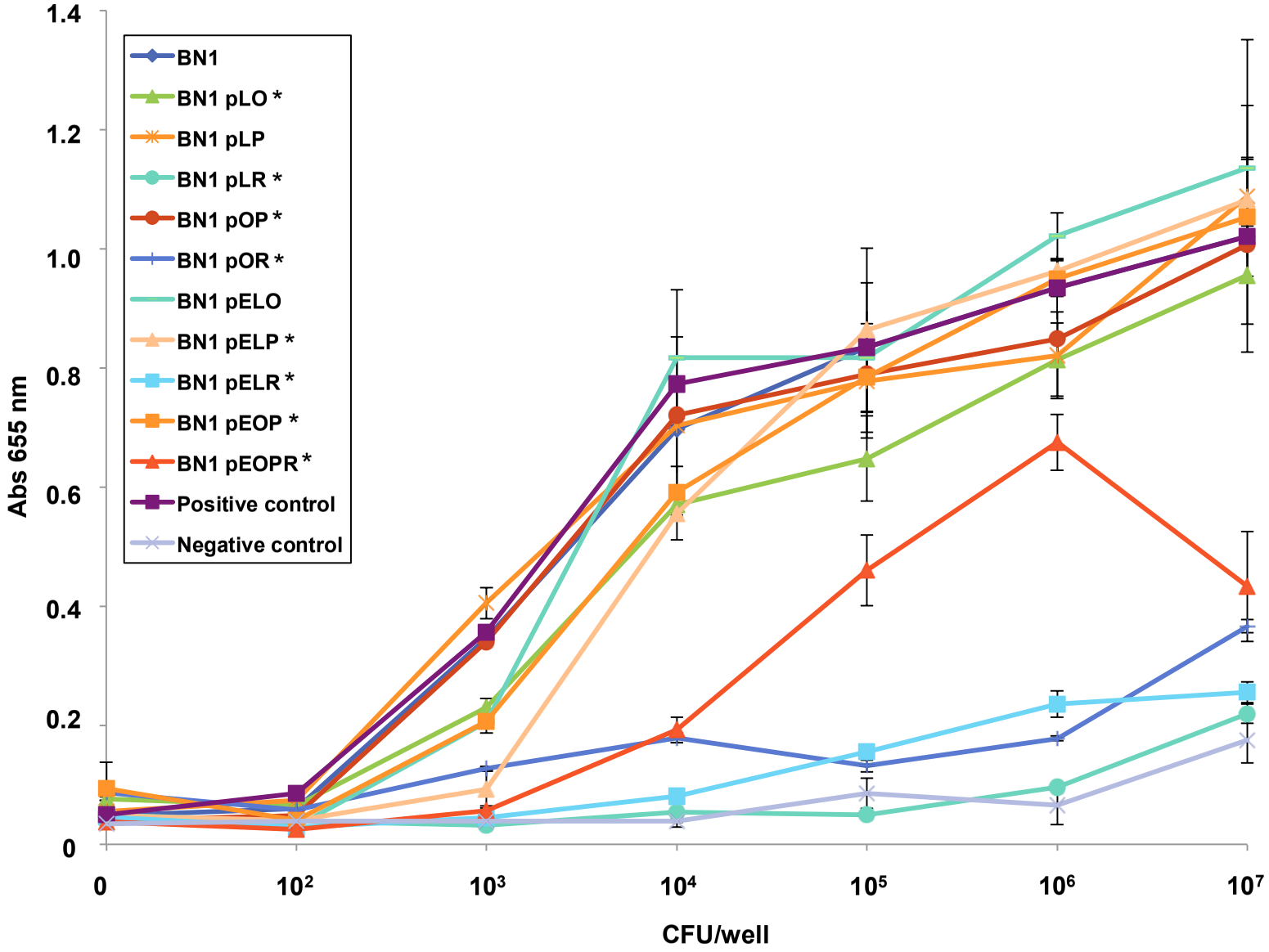
1.4
1.2
1.0
0.8
0.6
0.4
0.2
0
Abs 655 nm
BN1
BN1 pLO *
BN1 pLP
BN1 pLR *
BN1 pOP *
BN1 pOR *
BN1 pELO
BN1 pELP *
BN1 pELR *
BN1 pEOP *
BN1 pEOPR *
Positive control
Negative control
0
10²
10³
10⁴
10⁵
10⁶
10⁷
CFU/well

a, cont'd

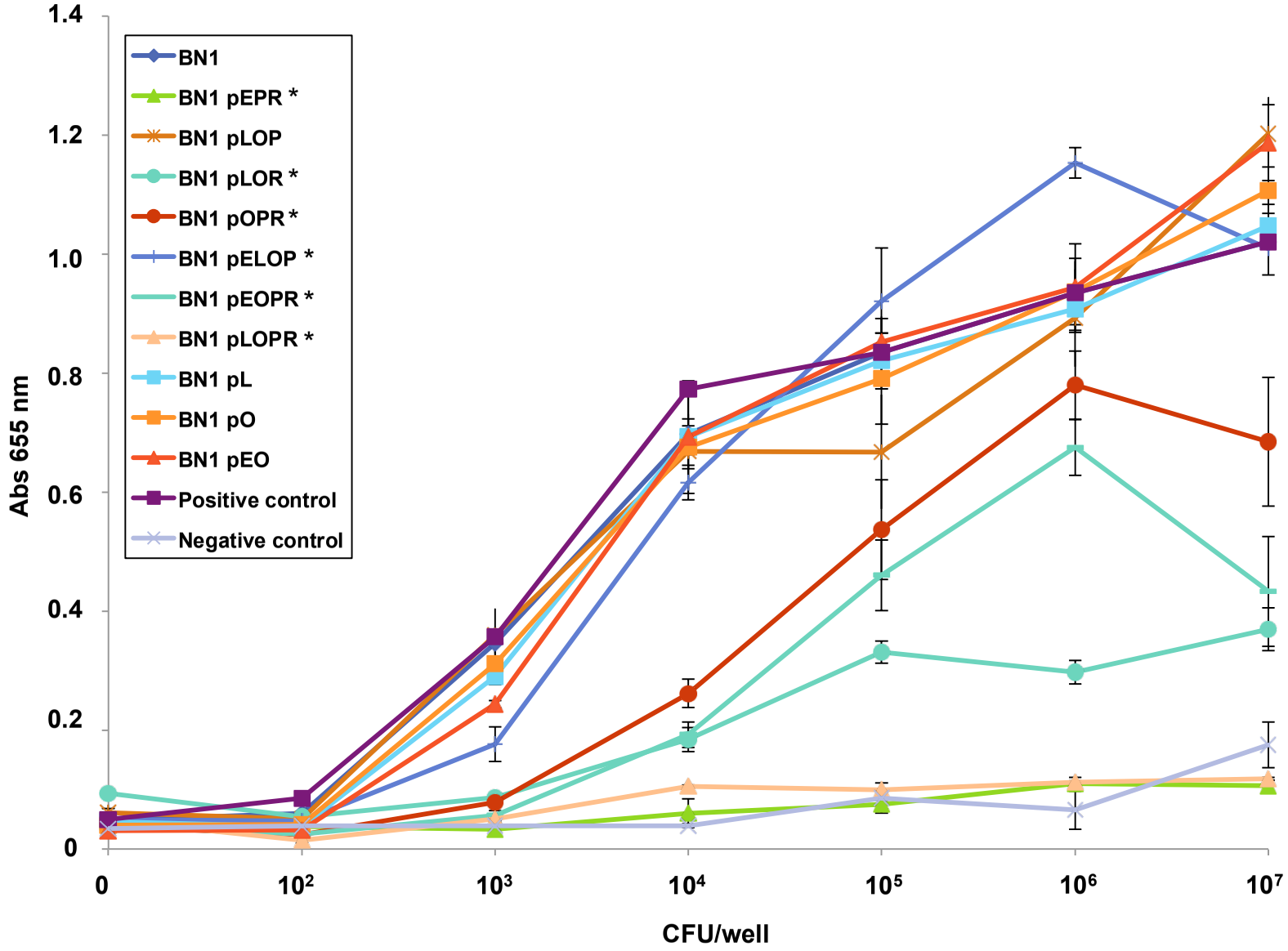
1.4
1.2
1.0
0.8
0.6
0.4
0.2
0
Abs 655 nm
BN1
BN1 pEPR *
BN1 pLOP
BN1 pLOR *
BN1 pOPR *
BN1 pELOP *
BN1 pEOPR *
BN1 pLOPR *
BN1 pL
BN1 pO
BN1 pEO
Positive control
Negative control
0
10^2
10^3
10^4
10^5
10^6
10^7
CFU/well

b

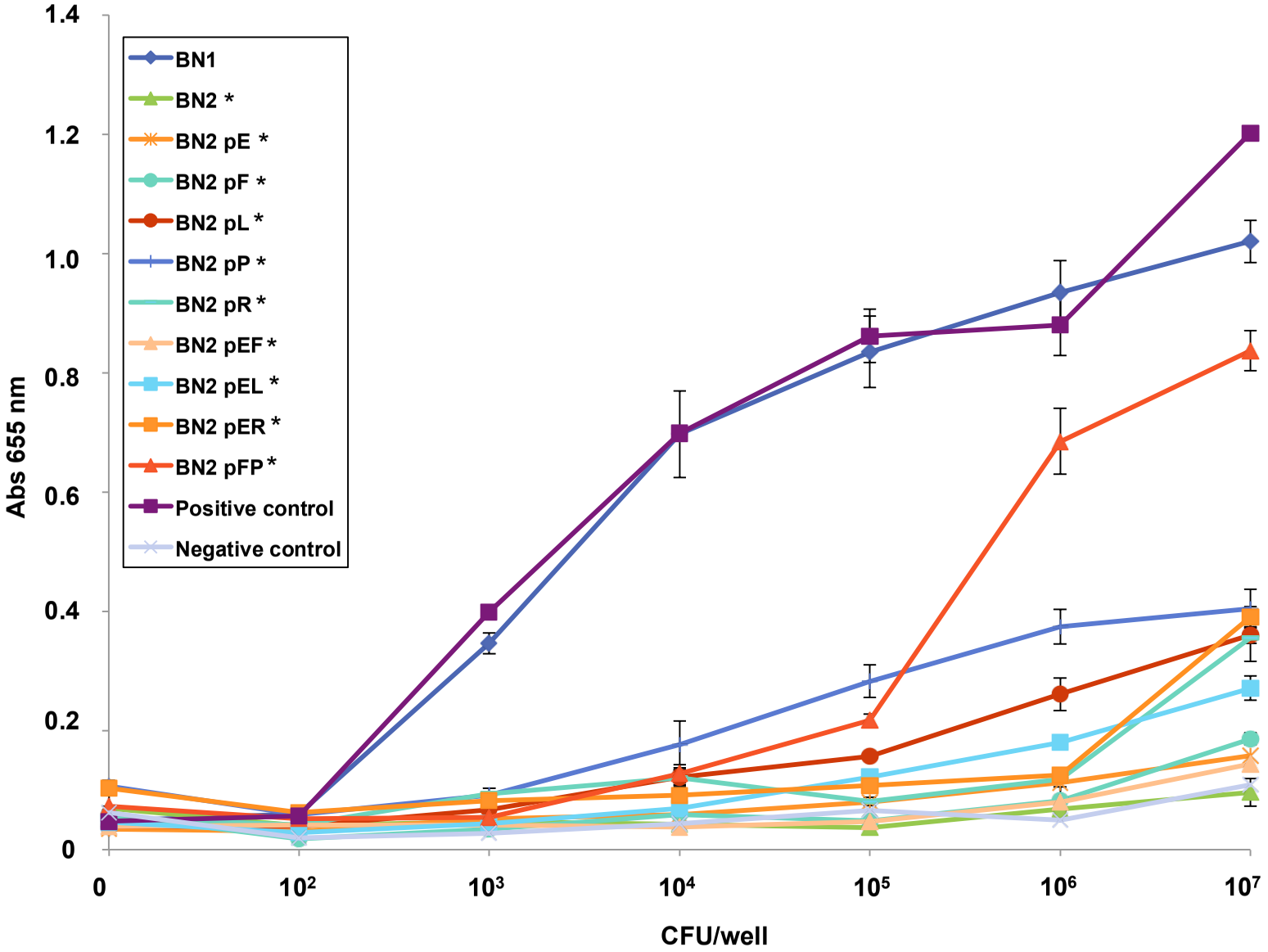
1.4
1.2
1.0
0.8
0.6
0.4
0.2
0
Abs 655 nm
BN1
BN2 *
BN2 pE *
BN2 pF *
BN2 pL *
BN2 pP *
BN2 pR *
BN2 pEF *
BN2 pEL *
BN2 pER *
BN2 pFP *
Positive control
Negative control
0
10²
10³
10⁴
10⁵
10⁶
10⁷
CFU/well

b, cont'd

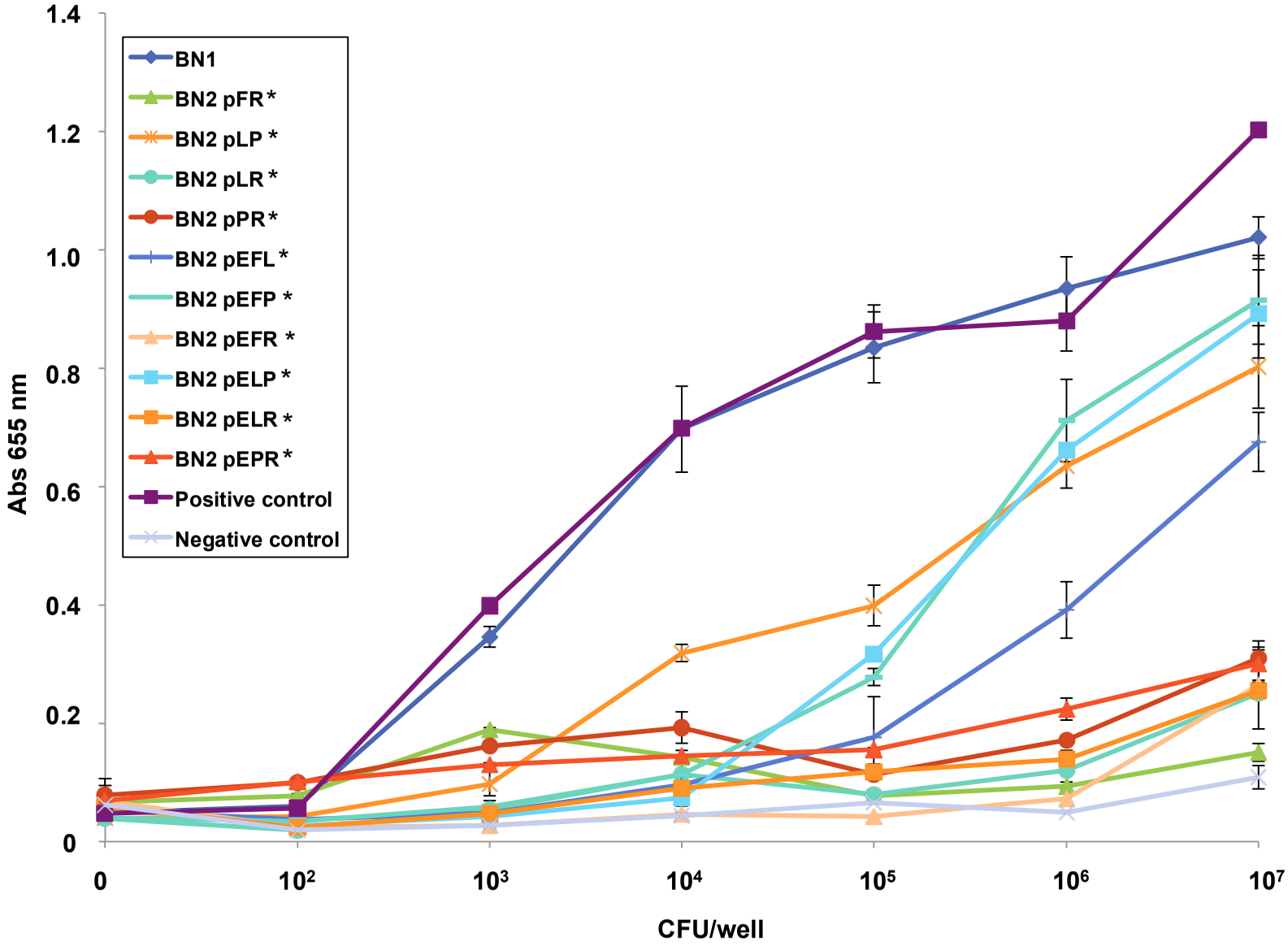
1.4
1.2
1.0
0.8
0.6
0.4
0.2
0
Abs 655 nm
BN1
BN2 pFR*
BN2 pLP *
BN2 pLR *
BN2 pPR*
BN2 pEFL *
BN2 pEFP *
BN2 pEFR *
BN2 pELP *
BN2 pELR *
BN2 pEPR*
Positive control
Negative control
0
10²
10³
10⁴
10⁵
10⁶
10⁷
CFU/well

b, cont'd

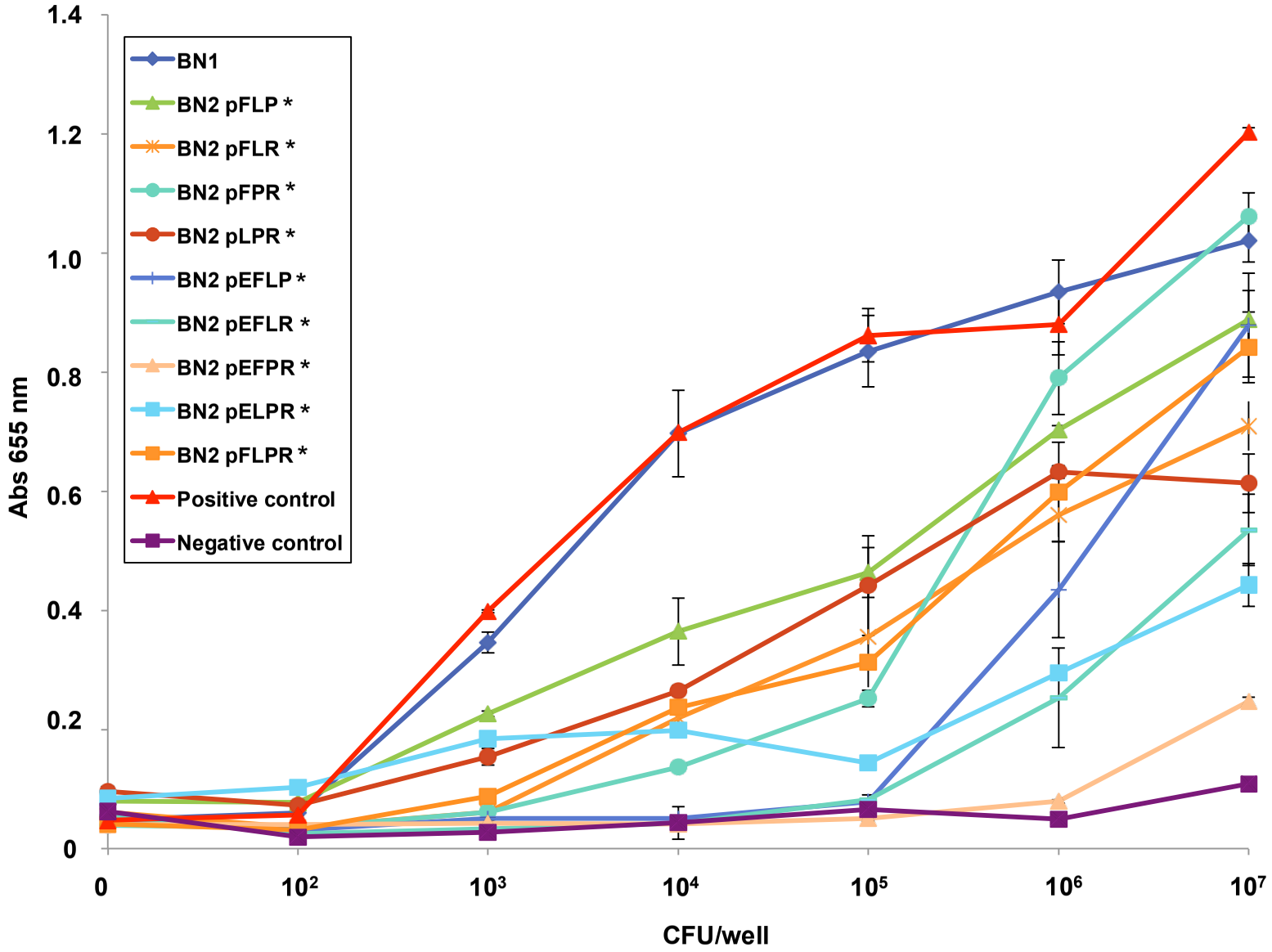
1.4
1.2
1.0
0.8
0.6
0.4
0.2
0
Abs 655 nm
BN1
BN2 pFLP *
BN2 pFLR *
BN2 pFPR *
BN2 pLPR *
BN2 pEFLP *
BN2 pEFLR *
BN2 pEFPR *
BN2 pELPR *
BN2 pFLPR *
Positive control
Negative control
0
10^2
10^3
10^4
10^5
10^6
10^7
CFU/well

c

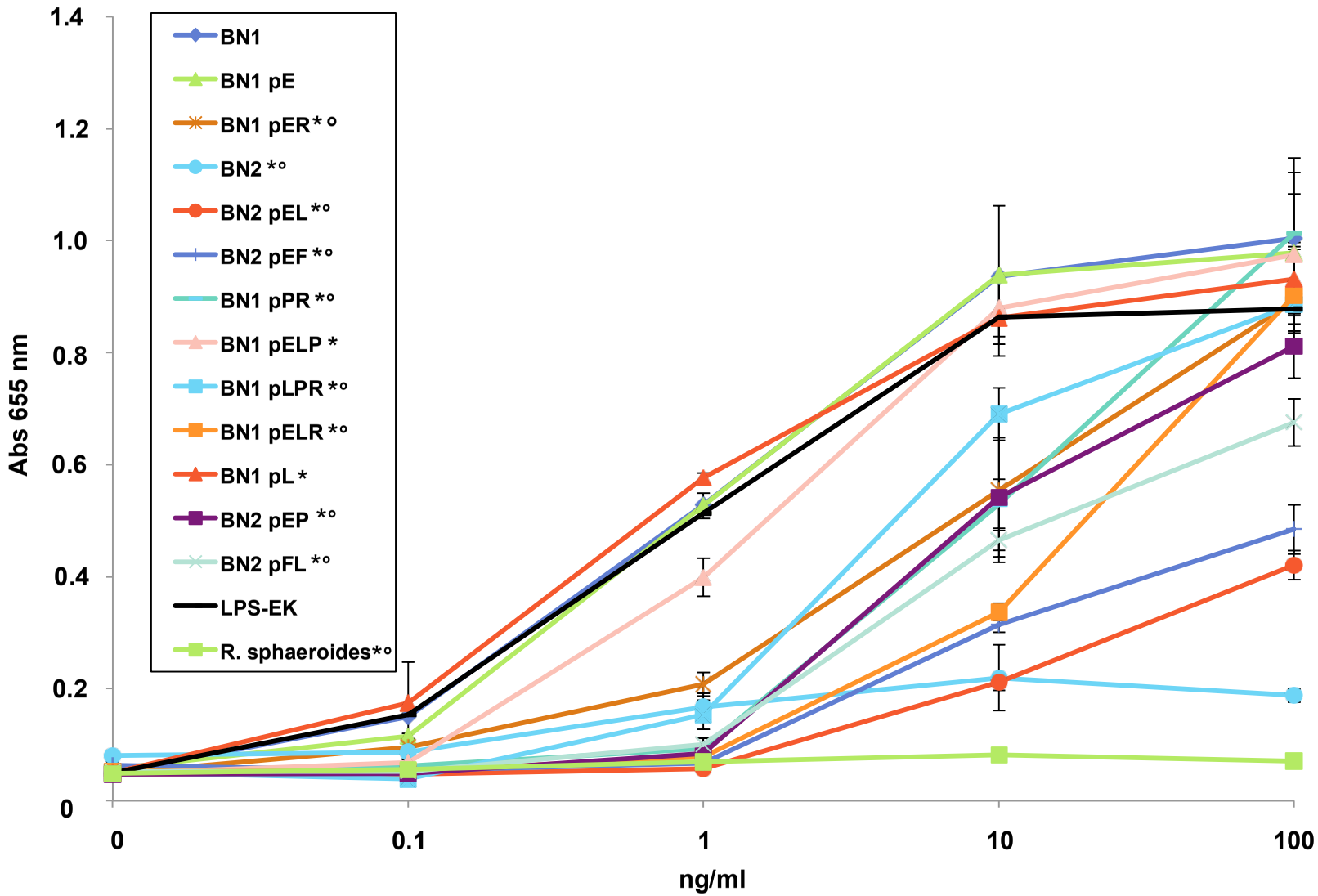
1.4
1.2
1.0
0.8
0.6
0.4
0.2
0
Abs 655 nm
0
0.1
1
10
100
ng/ml
BN1
BN1 pE
BN1 pER* °
BN2 *°
BN2 pEL *°
BN2 pEF *°
BN1 pPR *°
BN1 pELP *
BN1 pLPR *°
BN1 pELR *°
BN1 pL *
BN2 pEP *°
BN2 pFL *°
LPS-EK
R. sphaeroides*°

Fig. S5. Graphical representation of TLR4 stimulation by whole bacterial cells and LPS. All TLR4 data used to generate the colorimetric scale presented in Figure 2c is graphed here. a) TLR4 stimulation is shown of all strains in the BN1 background. These are split into three graphs due to number of samples. Significance is indicated by an asterisk and the p-values for samples that are significantly different from the BN1 background strain are listed below. First graph: pR, $1.98x10^{-7}$; pEL, .001; pER, $8.38x10^{-7}$; pELOR, $9.02x10^{-7}$; pELPR, 1.17-10^{-6}; pPR, $1.12x10^{-6}$; pLPR, $8.25x10^{-6}$. Second graph: pLO, .001; pLR, $1.77x10^{-6}$; pOR, $7.46x10^{-7}$; pELP, .003; pELR, $3.26x10^{-7}$; pEOP, .008; pEOPR, $3.26x10^{-6}$. Third graph: pEPR, $1.70x10^{-6}$; pLOR, $2.68x10^{-6}$; pOPR, $7.97x10^{-6}$; pELOP, .007; pEOPR, $3.26x10^{-6}$; pLOPR, $3.17x10^{-7}$. b) TLR4 stimulation is shown of all strains in the BN2 background, split into three graphs due to number of samples. The p-values for the significantly different samples follow. First graph: BN2, $2.06x10^{-7}$; pE, $2.32x10^{-7}$; pF, $2.39x10^{-7}$; pL, $7.46x10^{-7}$; pP, $1.55x10^{-5}$; pR, $7.7x10^{-7}$; pEF, $2.03x10^{-7}$; pEL, $2.94x10^{-7}$; pER, $6.95x10^{-7}$; pFP, $1.00x10^{-6}$. Second graph: pFR, $4.16x10^{-7}$; pLP, $4.88x10^{-6}$; pLR, $5.26x10^{-7}$; pPR, 5.65 $x10^{-6}$; pEFL, $6.70x10^{-6}$; pEFP, $3.02x10^{-6}$; pEFR, $2.20x10^{-7}$; pELP, $3.42x10^{-7}$; pELR, $8.33x10^{-7}$; pEPR, $6.01x10^{-7}$. Third graph: pFLP, $3.14x10^{-4}$; pFLR, $3.36x10^{-6}$; pFPR, $4.89x10^{-7}$; pLPR, $1.62x10^{-6}$; pEFLP, $2.25x10^{-7}$; pEFLR, $3.02x10^{-7}$; pEFPR, $2.08x10^{-7}$; pELPR, $9.88x10^{-7}$; pFLPR, $8.68x10^{-6}$. c) TLR4 stimulation with LPS is shown. The p-values for the significantly different samples at 1 ng/ml LPS follow, and are indicated by asterisks: BN1 pL, $9.4x10^{-3}$; BN1 pELP, $2.3x10^{-3}$; BN1 pPR, $1.42x10^{-6}$; BN1 pELR, $1.60x10^{-6}$; BN1 pLPR, $1.84x10^{-5}$; BN1 pER, $2.16x10^{-5}$; BN2 pEP, $1.1x10^{-5}$; BN2 pFL, $2.89x10^{-6}$; BN2 pEF, $1.43x10^{-6}$; BN2 pEL, $1.05x10^{-5}$; BN2, $1.95x10^{-5}$. P-values at 10 ng/ml are indicated by BN1 pPR, $3.67x10^{-4}$; BN1 pELR, $4.12x10^{-5}$; BN1 pLPR, $2.65x10^{-3}$; BN1 pER, $4.93x10^{-3}$; BN2 pEP, $2.58x10^{-3}$; BN2 pFL, $1.10x10^{-4}$; BN2 pEF, $3.48x10^{-5}$; BN2 pEL, $1.94x10^{-5}$; BN2, $6.53x10^{-5}$

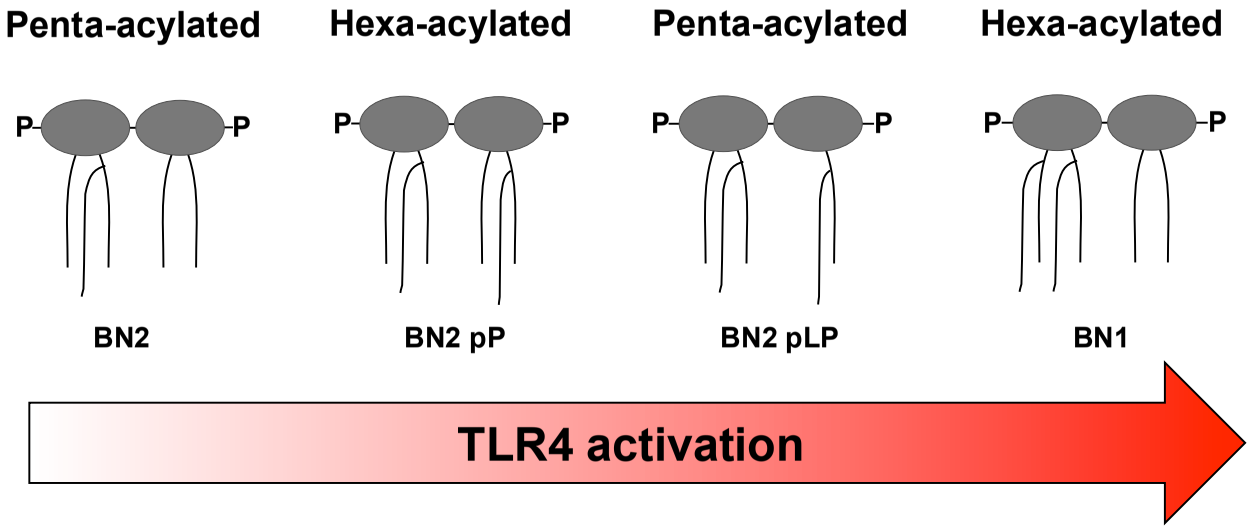

Fig. S6. An example of the effect of acyl chain position on TLR4 activation. BN2, which is penta-acylated, is unstimulatory. Expression of PagP in the BN2 strain increases stimulation. Including PagL expression, in BN2 pLP, further increases stimulation, even though more lipid A molecules are then penta-acylated.

Fig. S7, a

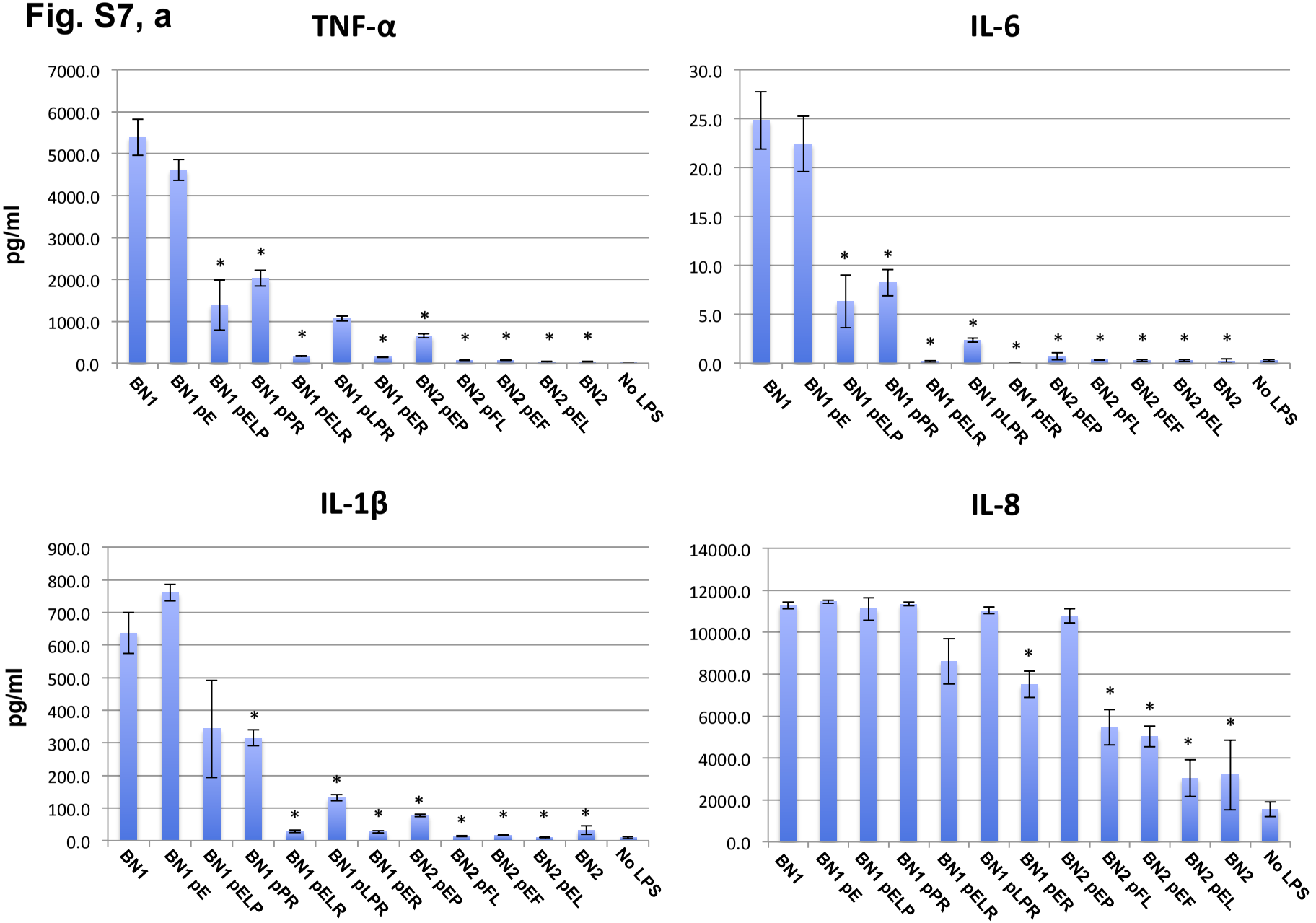
TNF-α
pg/ml
7000.0
6000.0
5000.0
4000.0
3000.0
2000.0
1000.0
0.0
BN1
BN1 pE
BN1 pELP
BN1 pPR
BN1 pELR
BN1 pLPR
BN1 pER
BN2 pEP
BN2 pFL
BN2 pEF
BN2 pEL
BN2
No LPS
IL-6
30.0
25.0
20.0
15.0
10.0
5.0
0.0
IL-1β
900.0
800.0
700.0
600.0
500.0
400.0
300.0
200.0
100.0
0.0
IL-8
14000.0
12000.0
10000.0
8000.0
6000.0
4000.0
2000.0
0.0

b

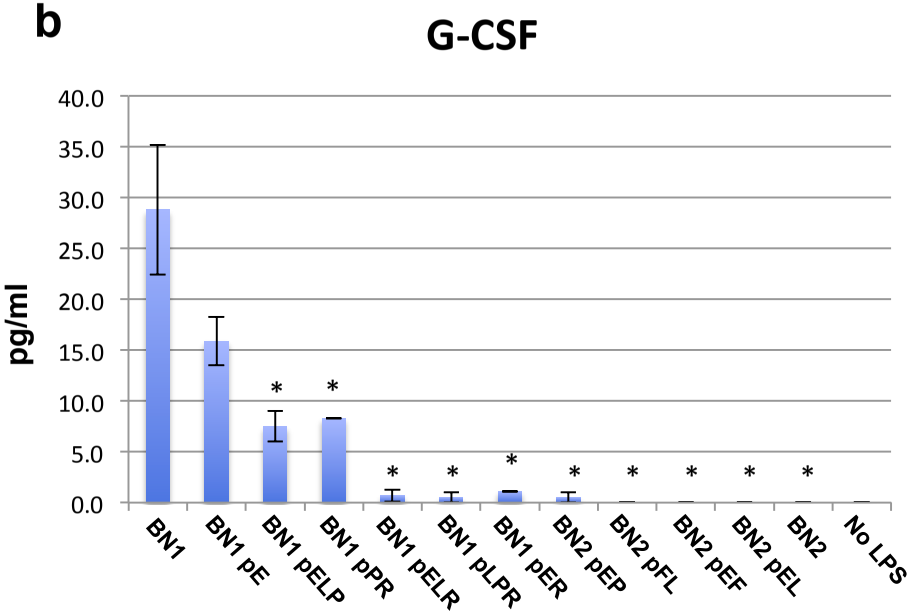
G-CSF
pg/ml
40.0
35.0
30.0
25.0
20.0
15.0
10.0
5.0
0.0
BN1
BN1 pE
BN1 pELP
BN1 pPR
BN1 pELR
BN1 pLPR
BN1 pER
BN2 pEP
BN2 pFL
BN2 pEF
BN2 pEL
BN2
No LPS

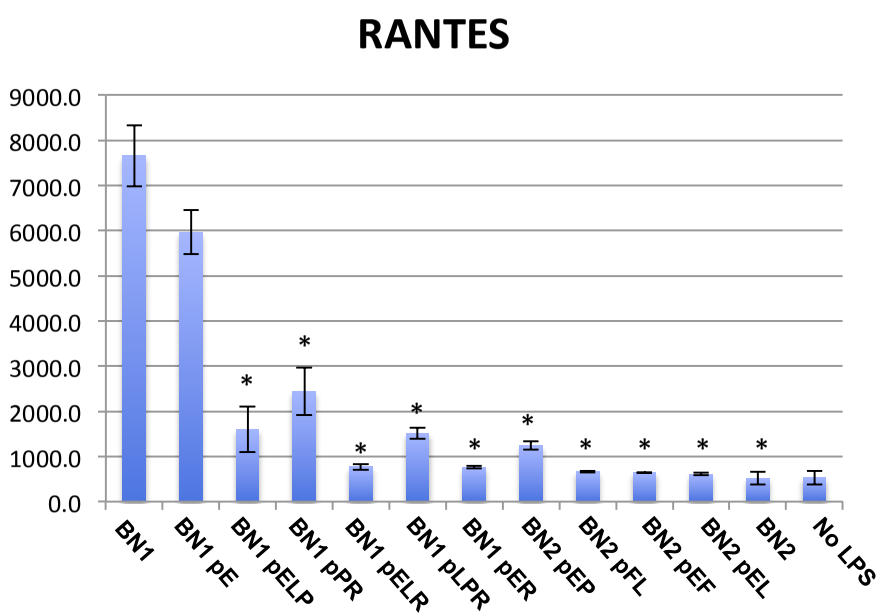
RANTES
9000.0
8000.0
7000.0
6000.0
5000.0
4000.0
3000.0
2000.0
1000.0
0.0
BN1
BN1 pE
BN1 pELP
BN1 pPR
BN1 pELR
BN1 pLPR
BN1 pER
BN2 pEP
BN2 pFL
BN2 pEF
BN2 pEL
BN2
No LPS

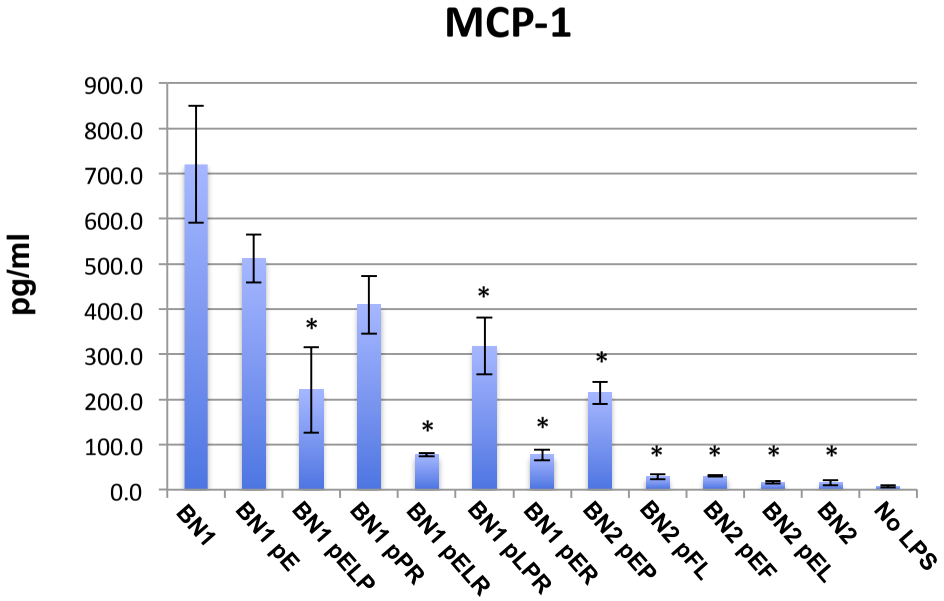
MCP-1
pg/ml
900.0
800.0
700.0
600.0
500.0
400.0
300.0
200.0
100.0
0.0
BN1
BN1 pE
BN1 pELP
BN1 pPR
BN1 pELR
BN1 pLPR
BN1 pER
BN2 pEP
BN2 pFL
BN2 pEF
BN2 pEL
BN2
No LPS

c

	BN1 pE	BN1 pER	BN1 pELP	BN1 pELR	BN1 pPR	BN1 pLPR	BN2	BN2 pEF	BN2 pEL	BN2 pFL	BN2 pEP
G-CSF	3.01E-02	6.21E-07	4.89E-03	1.64E-03	1.89E-05	1.63E-03	4.38E-07	4.38E-07	4.38E-07	4.38E-07	1.63E-03
IL-1B	3.57E-02	7.77E-05	3.49E-02	7.84E-05	1.22E-03	1.68E-04	8.65E-05	7.19E-05	6.89E-05	7.06E-05	1.09E-04
IL-6	3.74E-01	6.20E-10	1.33E-03	1.35E-04	8.93E-04	1.93E-04	1.36E-04	1.36E-04	1.36E-04	7.14E-10	1.49E-04
IL-8	1.40E-01	5.42E-04	6.30E-01	1.34E-02	5.50E-01	1.38E-01	1.10E-03	3.17E-05	8.84E-05	3.02E-04	7.95E-02
MCP-1	6.23E-02	1.03E-03	5.78E-03	1.01E-03	2.03E-02	8.45E-03	7.15E-04	7.73E-04	7.16E-04	7.67E-04	2.67E-03
RANTES	2.49E-02	6.06E-05	2.39E-04	6.15E-05	4.64E-04	1.02E-04	5.72E-05	5.63E-05	5.54E-05	5.70E-05	8.32E-05
TNF-a	5.38E-02	3.04E-05	7.21E-04	3.10E-05	2.50E-04	6.77E-05	2.80E-05	2.87E-05	2.81E-05	2.88E-05	4.70E-05

Fig. S7. Cytokine analysis of THP-1 cells exposed to LPS.
All individual cytokine data used to generate Figure 5b and c is presented here in picograms/ml. Asterisks indicate statistical significance with a P value < 0.01 (a) Cytokines induced by the MyD88 pathway: TNF-α, IL-6, IL-1β, and IL-8. (b) Cytokines induced by the Trif pathway: G-CSF, RANTES, MCP-1. (c) P values of all samples are compared to BN1.

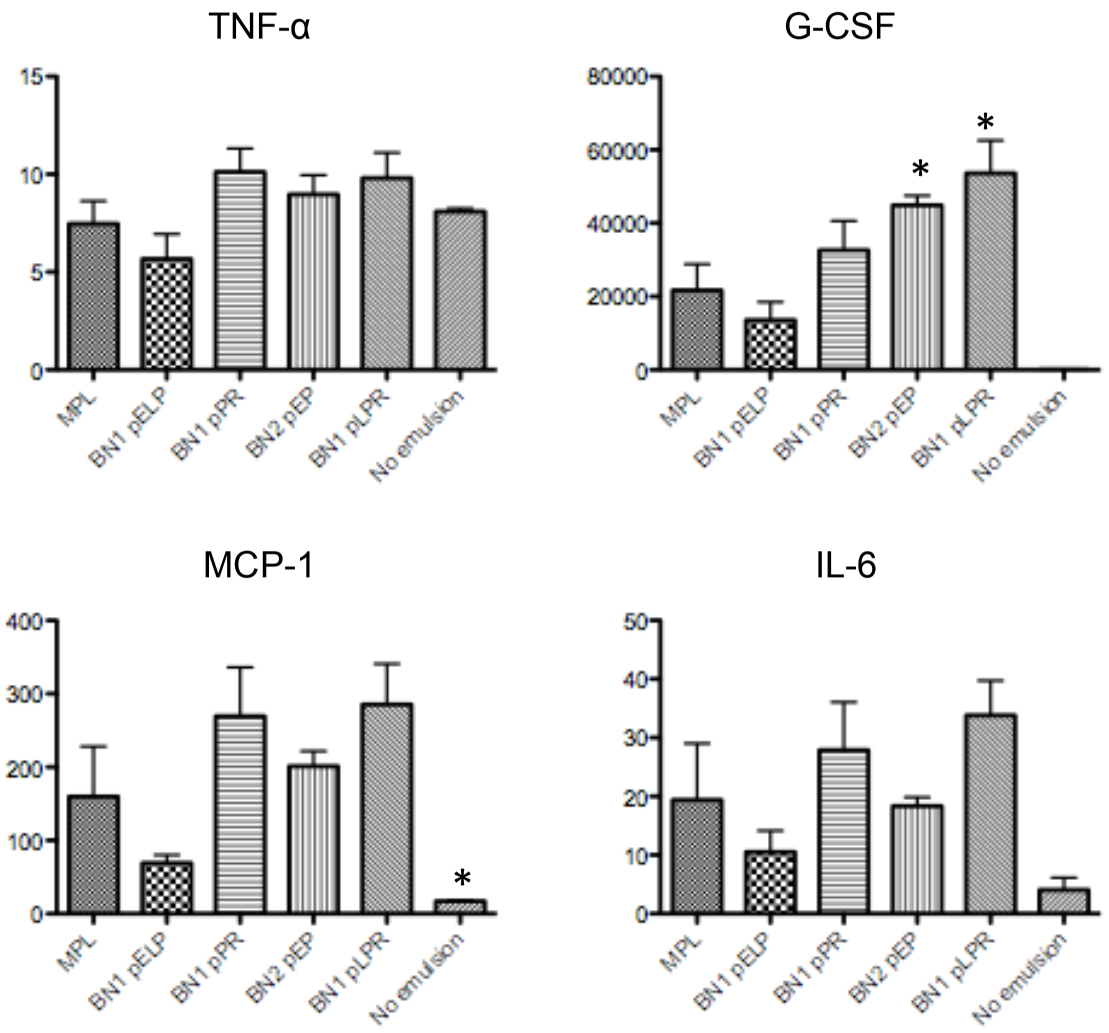

Fig. S8. Cytokine analysis of serum from immunized mice. Immunized mice were bled 24 hours after final immunization and cytokine levels in serum were measured by Luminex.

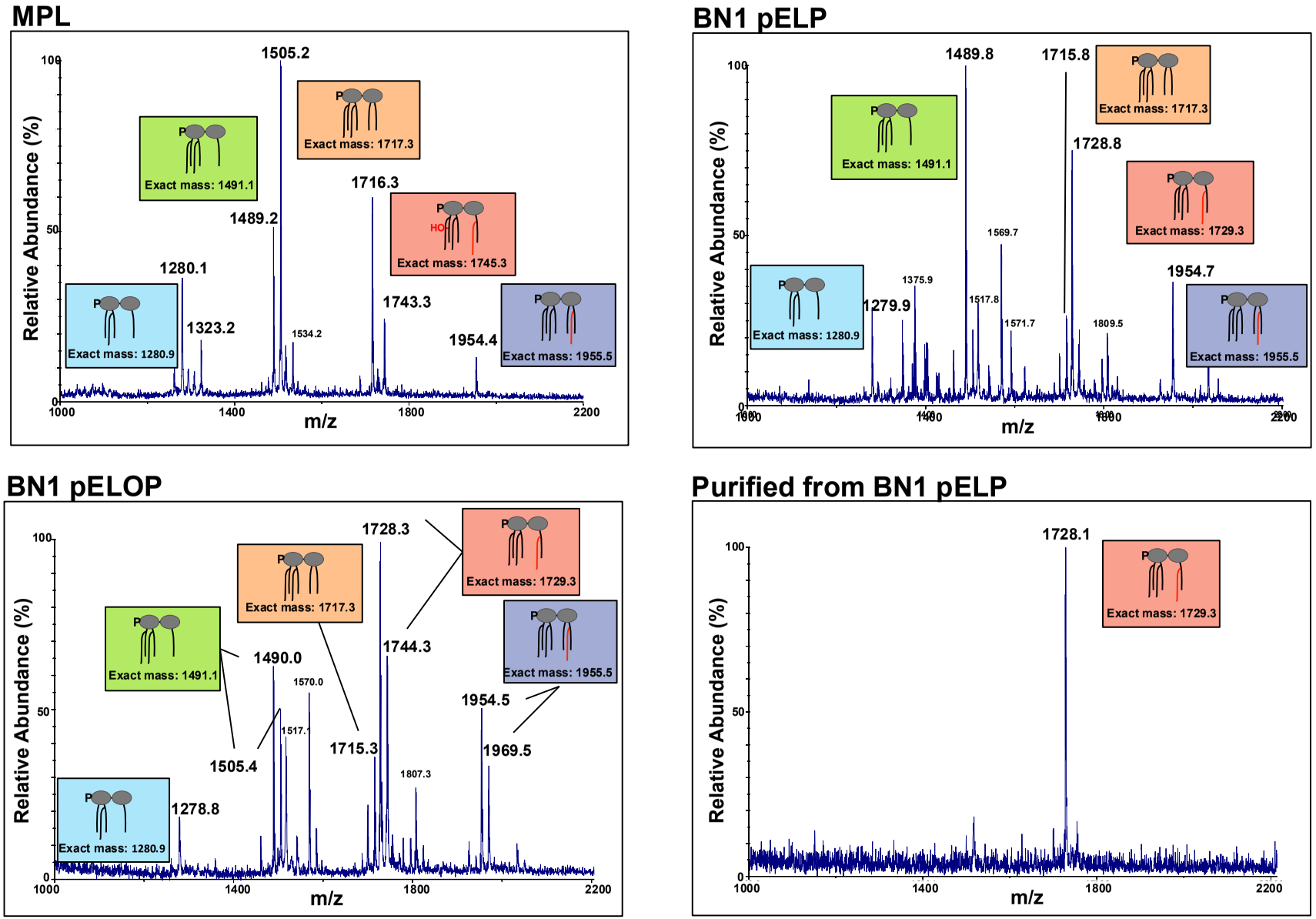

Fig. S9. MS of engineered strains compared to MPL from *S. minnesota*. MS data is presented of MPL from *S. minnesota,* the two strains from the library that produce similar profiles, even without additional chemical treatment, and the purified 3-*O*-deacyl-4′-monophosphoryl lipid A. Colored boxes indicate structures with the same phosphorylation and acyl chain patterns. Red box indicates the hydroxylated and nonhydroxylated 3-*O*-deacyl-4′-monophosphoryl lipid A, the most notable species of MPL.

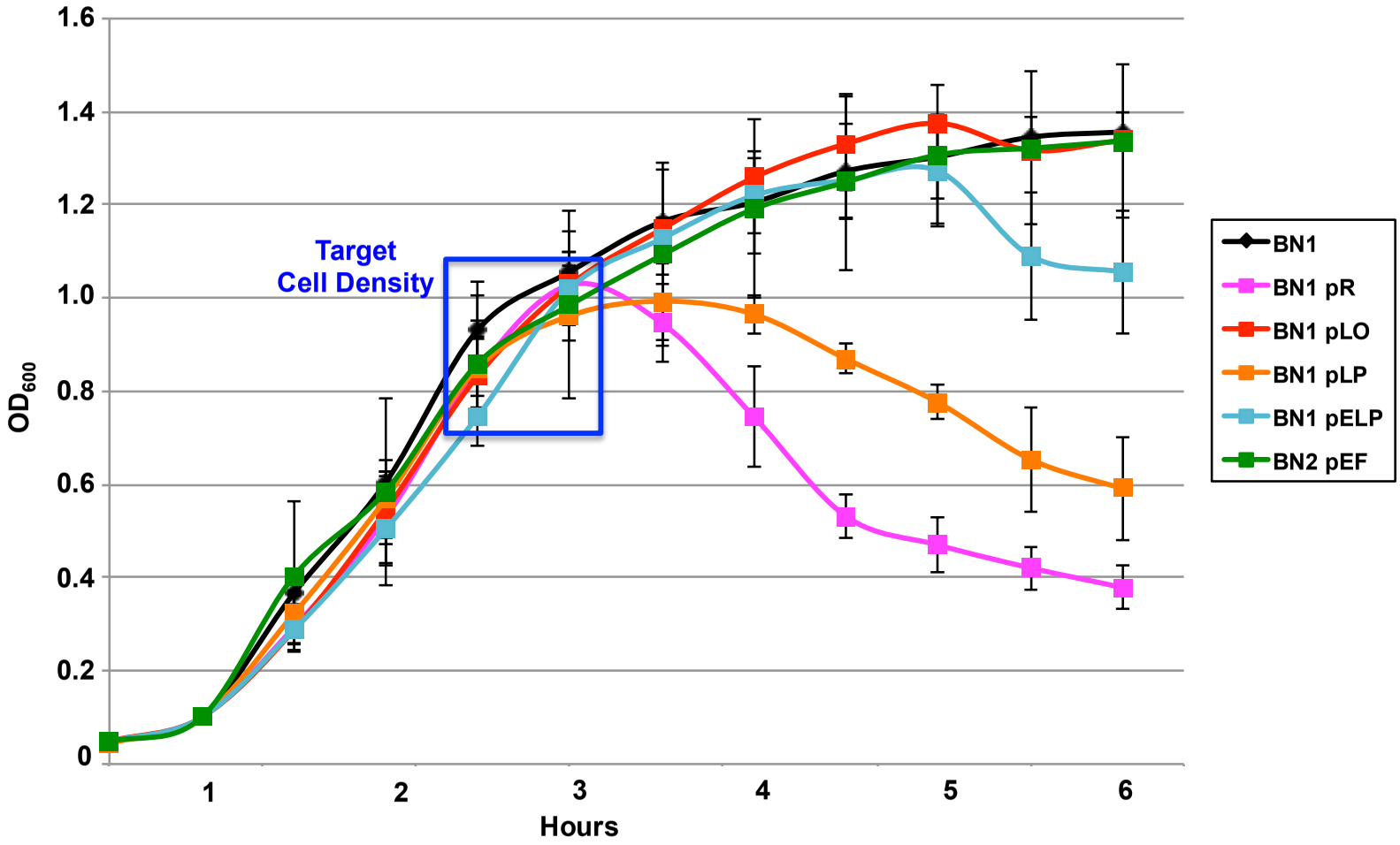

Fig. S10. Growth curves of engineered strains. An example graph is shown that represents the growth curve of the strains. All 61 strains reach an OD600 of at least 0.8, although many do not survive stationary phase, as represented by strain BN1 pR in purple. The background strain, BN1 is shown in black. The blue square indicates the target cell density when cells were harvested for experiments.